A STUDY OF THE PENETRATION OF PHOTOVOLTAICS INTO THE LIBYAN POWER SYSTEM

By

ABDULMUNIM HADI MABROUK GUWAEDER

Bachelor of Engineering in Electrical and Electronics Engineering
Higher Institute of Surman
Surman, Libya
1992

Master of Engineering in Electrical and Computer Engineering
Newcastle Upon Tyne University
Newcastle, United Kingdom
2003

Submitted to the Faculty of the
Graduate College of the
Oklahoma State University
in partial fulfillment of
the requirements for
the Degree of
DOCTOR OF PHILOSOPHY
December, 2018

A STUDY OF THE PENETRATION OF PHOTOVOLTAICS INTO THE LIBYAN POWER SYSTEM

Dissertation Approved:

Dr. R Ramakumar

Dissertation Advisor

Dr. Nishantha Ekneligoda

Dr. Qi Cheng

Dr. Sundar V. Madihally

ACKNOWLEDGMENTS

One of the most rewarding achievements in my life to date is the completion of my doctoral: "Dissertation" at Oklahoma State University. I would like to take this opportunity to convey my immense gratitude and profound respect to my advisor, Dr. R Ramakumar, for his invaluable guidance, patience and provided insight into many of the problems that were encountered. His positive attitude throughout the duration of this dissertation always put things into perspective whenever difficulties arose. This dissertation would not have been possible without him.

My deepest gratitude to my committee members, Dr. Nishantha Ekneligoda, Dr. Qi Cheng and Dr. Sundar V. Madihally for their brilliant help, comments and valuable suggestions have been extremely beneficial towards my research.

I also would like to acknowledge the financial support by the Libyan Government of my home country and the Oklahoma State University Engineering Energy laboratory and the PSO/Albrecht Naeter Professorship in the School of Electrical And Computer Engineering.

There are many other people that have contributed directly or indirectly to this dissertation. Some acted as sounding boards, sources of information, or providing resources that contributed to the development of my dissertation. while their individual contributions have been small, their efforts have still been greatly appreciated.

I dedicate this dissertation and my degree to all members of my family, especially my father, mother, wife and children for keeping me sane.

I have greatly appreciated the help of Nancy Crenshaw and Helen Daggs who gave their full assistance whenever needed.

Finally, I would like to thank my colleagues and friends who supported me along the way.

Acknowledgements reflect the views of the author and are not endorsed by committee members or Oklahoma State University.

Name: ABDULMUNIM HADI MABROUK GUWAEDER

Date of Degree: DECEMBER, 2018

Title of Study: A STUDY OF THE PENETRATION OF PHOTOVOLTAICS INTO THE LIBYAN POWER SYSTEM

Major Field: ELECTRICAL AND COMPUTER ENGINEERING

Abstract: The purpose of this study is to investigate the impacts of the penetration of Photovoltaic (PV) power generation on the Libyan power system with reference to voltage profile improvement and overall system performance. Integration of solar power generation with the Libyan electric power grid would provide a boost to the generation of clean electricity by harnessing renewable energy resources. Such an approach will reduce greenhouse gas GHG emissions by supplying zero-emission solar power to the grid and thereby mitigating overall CO2 emissions. The many advantages of integration of PV are lower fuel consumption and less reliance on traditional fuel sources, clean energy, less operation and maintenance cost as compared to diesel generators and the possibility of exporting the saved fuel to enhance the economic health of Libya. This dissertation presents a brief description of the Libyan power system with its past, current state of generation, transmission infrastructure and potential solar power plans. Further, this dissertation has considered several solar energy scenarios for Libya, modeling of solar irradiation for a few locations considered in this study and the impact of solar PV generation on the voltage profile and overall performance of the Libyan electric power grid.

TABLE OF CONTENTS

LIST OF TABLES

LIST OF FIGURES

NOMENCLATURE

HVDC	High voltage direct current
PV	Photovoltaic
CSP	Concentrating thermal power
STE	Solar thermal electricity
GECOL	General electric company of Libya
CSES	Center for solar energy studies
I_{sc}	Short circuit current (A)
D_j	Nonlinear function (diode) impedance
R_{sh}	Shunt resistance
R_s	Series resistance
R_L	Resistive load
K_1	Short circuit temperature coefficient (A/°C)
NCOT	Nominal Cell Operating Temperature (°C) provided by the manufacture
V_{oc}	Open circuit voltage (V)
P_{out}	the electrical output power of the cell (W)
P_{in}	The input power of the cell
η_{Max}	The maximum cell Efficiency
P_s	The solar radiation level per unit area
A_s	The active cell area
I_{mp}	Current at maximum power point
V_{mp}	Voltage at maximum power point
$I(t)$	The output current at time t, Amp

$V(t)$	The output voltage at time t, Volt
A	The ideality factor for p-n junction
$T(t)$	The temperature at time t, Kelvin
KB	The Boltzman's constant in Joules per Kelvin, $1.38 * 10^{-23} J/k$
q	The charge of the electron in Coulombs, $1.6 * 10^{-19} C$
$I_O(t)$	The reverse saturation current at time t, Amp
T_r	The reference temperature, oK
E_{go}	The band-gap energy of the semiconductor used in solar cells module
K_I	The short circuit current temperature coefficient
I_{or}	The saturation current at Tr, Amp
$H_T(t)$	The average hourly radiation on the tilted surface,kW/m^2
$f(x)$	The probability density function
β	Shape parameter ($kWh/m^2/day$)
α	Scale parameter ($kWh/m^2/day$)
μ and σ	The mean and standard deviation
χ^2	Chi-squared test
O_i	The observed frequency
E_i	The expected frequency
$F(x)$	The corresponding cumulative distribution
$C.V$	Critical value
x_U, x_L	The lower and upper limits of the i^{th} bin
KS	Kolmogorov Smirnov test
$F_o[x_i]$	Observed cumulative distribution function
$F_T[x_i]$	Hypothesized cumulative distribution function
RMSE	Root mean square error
R	Correlation coefficient

OPF	Optimal power flow
δ	phase angle of voltage
P	Active power
Q	Reactive power
$HRSG$	Heat recovery steam generator
P_{say}	output power of the PV module during state y;
N	Number of modules;
FF	Fill factor;
V_y	voltage during state y
I_y	current during state y
V_{MPP}	Voltage corresponding to the maximum power point
I_{MPP}	Current corresponding to the maximum power point
T_{cy}	Cell temperature $^{\circ}C$ during state y
T_A	Ambient temperature $^{\circ}C$
K_i	Current temperature coefficient $A/^{\circ}C$
K_v	Voltage temperature coefficient $V/^{\circ}C$
N_{OT}	Nominal operating temperature of cell in $^{\circ}C$
S_{ay}	Average solar irradiance of state y
CF	Capacity factor
(Pr_n)	Probability density function
V_{index}	Voltage index

CHAPTER 1

INTRODUCTION

1.1 Background

It is well known that the electric power grid is a network of electrical components deployed to supply, transfer, store, and consume electricity over an extended area. A power system consists of generators that generate power, a transmission system that carries the power from the generating centers, and a distribution system that supplies power to nearby homes and industries. Smaller power systems are also found in industrial settings, hospitals, commercial buildings and homes. The majority of these systems rely upon three-phase AC power, the standard for large-scale power transmission and distribution across modern world. Specialized power systems that do not always rely upon three-phase AC power are found in aircraft, electric rail systems, ocean liners and automobiles. Developments in power systems continued beyond the nineteenth century. In 1936, the first experimental HVDC (high voltage direct current) line using mercury arc valves was built between Schenectady and Mechanicville, in New York [1]. HVDC had previously been achieved by series-connected direct current generators and motors, although these suffered from serious reliability issues [1, 2].

The uses of energy have evolved as humans have changed patterns of energy consumption. Renewable resources such as wind, insolation, water, and biomass were the first sources of energy tapped to provide heat, light, and usable power. The energy stored in fossil fuels (coal, oil and natural gas) and, more recently, nuclear power fueled the vast expansion of global, industrial, residential, and transportation sectors during the

20th century [3]. However, as a result of population growth and the modern standard of living, fossil fuel consumption has also increased, and the concerns over energy security and the negative impacts of greenhouse gases on the environment have also risen. Volatilities in foreign energy markets affecting fuel prices and availability have long raised the issue of domestic energy security. In addition, recent concerns over the limited supply of fossil fuels and the negative impacts of greenhouse gases released by fossil-fuel combustion have spurred efforts to utilize renewables resources such as, wind, insolation, biomass, and geothermal heat to meet global energy demands. At this time, renewable sources of energy have considerable potential to reduce the negative impacts of current energy use and to increase the domestic resource base. The fundamental challenge is in collecting the energy in renewable resources and converting it to usable forms at the scales necessary to allow renewables to contribute significantly to domestic energy supply [3].

1.2 Renewable Energy

Renewable energy is defined as energy that comes from replenishable resources that are not significantly depleted by their use. Examples are insolation, wind, rain, tides, waves and geothermal heat. Renewables are rapidly becoming a significant component of mainstream sources of energy around the world. Rapid growth of renewable resource utilization is driven by several factors including improving cost-competitiveness, dedicated policy initiatives, better access to financing, concerns about energy security and the environment, growing demand for energy in developing and emerging economies, and the need for sustainability.

There are many countries already forging ahead towards a low-carbon future. In 2015, Sweden issued a challenge with an ambitious goal of eliminating fossil fuel usage within its borders, and immediately ramping up investment in solar, wind, energy

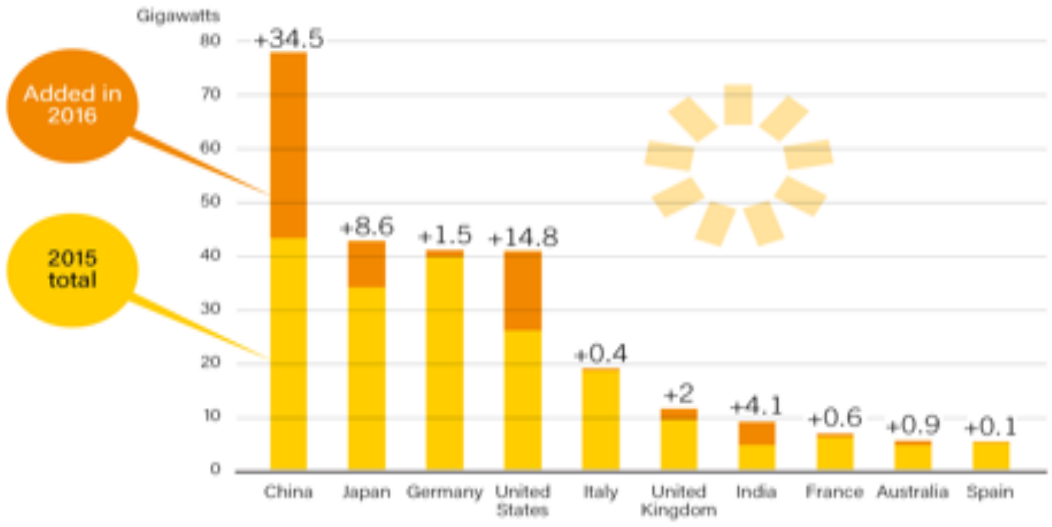

Figure 1.1: Solar PV capacity and additions, top 10 countries, 2016 [7]

storage, smart grids, and clean transport [4].

In 2015, 99% of Costa Rica's electricity came from renewables with its unique geography and commitment to environmental preservation. Although the country is small, it meets a significant portion of its energy needs using hydroelectric, geothermal, solar, wind and other low-carbon sources [5]. Germany set the trend in Europe when it comes to renewable energy and has the ability to meet as much of 78% of daily electricity demand from renewables. For a relatively cloudy country of over 80 million people, Germany is looking forward to a very bright future with solar energy utilization [6].

China, the world's largest carbon emitter is becoming a leader in renewable energy use. It may seem counter-intuitive, but in 2016 China had the most installed wind energy capacity by a longshot and the largest installed solar PV capacity as shown in Figure 1.1.

China has also committed to phasing out coal and cleaning up its polluted air. The development of concentrating solar thermal power (CSP), also known as solar thermal electricity (STE), in China will be around 10 GW by 2020, larger than the

global CSP installed capacity (4940 MW) in 2015 [8]. In 2016, with a high solar intensity, Morocco has started construction of one of the largest CSP on earth with a capacity of 500 MW housed in a three-plant Noor-Ouarzazate CSP complex [9]. This plant is expected to ultimately supply power to 1.1 million Moroccans by 2018 and reduce the country‘s energy dependence by about two and half million tons of oil, while also lowering carbon emissions by 760,000 tons per year [9].

In 2016, renewable technologies continued to attract far more investment dollars than did fossil fuel or nuclear power generating plants. An estimated USD 249.8 Billion was committed to constructing new renewable power plants (including USD 226.6 Billion excluding large-scale hydropower, plus an estimated USD 23.2 Billion for hydropower projects larger than 50 MW). This compares to approximately USD 113.8 Billion committed to fossil fuel-fired generating capacity and USD 30 Billion for nuclear power capacity [10].

1.3 Worldwide Use of Renewable Energy

The world now adds more renewable power capacity annually than capacity additions from all fossil fuels plants combined. In 2016, renewables accounted for an estimated more than 62% of net additions to global power generating capacity. By year‘s end, renewables comprised an estimated 28.9% of the world‘s power generating capacity, enough to supply an estimated 24.5% of global electricity, with hydropower providing about 16.6% as shown in Figure 1.2 [7].

During 2016, at least 75 GW of solar PV capacity was added worldwide - equivalent to the installation of more than 31,000 solar panels every hour. More solar PV capacity was installed in 2016 than the cumulative world capacity five years earlier. Based on the installed capacity of renewable energy sources at the end of 2016, global solar PV capacity totaled at least 303 GW [10] as illustrated in Figure 1.3.

Figure 1.2: Estimated Renewable Energy Share of Global Electricity Production by End of 2016 [7]

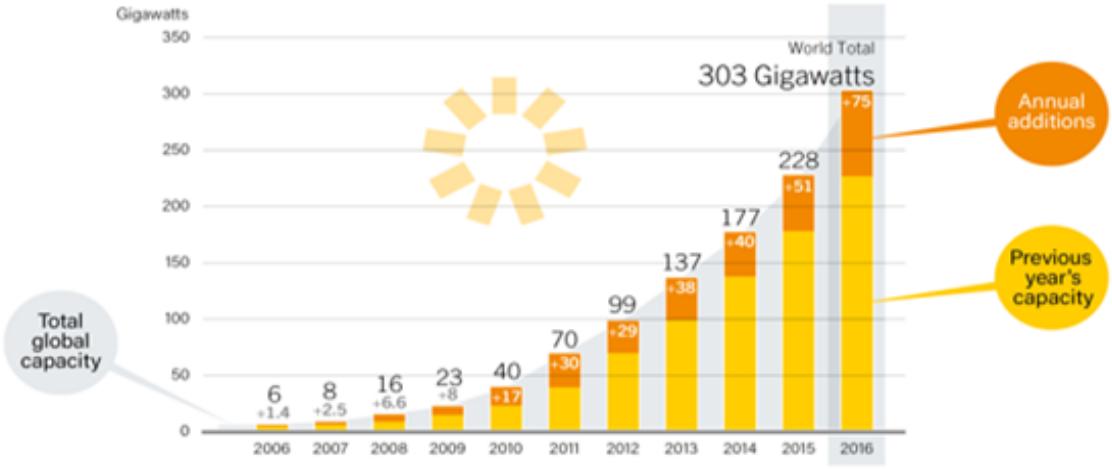

Figure 1.3: Solar PV global capacity and annual additions, 2006-2016 [10]

1.4 Impact of Variable Generation on the Power System

Increasing the amount of variable renewable resources on the grid adds additional supply variations and uncertainty, complicating the task of keeping production matched to load. Much more is known about wind generation and its impact on power system operations and flexibility requirements than for other variable resources. PV forecasting is not as mature a field as wind forecasting is, and statistics on geographic dispersion are not well developed. However, PV forecasting will likely use a combination of numerical weather prediction models, along with methods that quantity

disruptions in clear-skies estimate of insolation to simulate and forecast the impact of cloud cover. Today's power system has been designed to manage current levels of variability and uncertainty introduction of renewables will ersatz new challenges. Morning and evening load ramps can be significant, and system operators have established procedures to ensure that sufficient ramping capability is available. During the night and other low-load periods, baseload generators can be backed down and intermediate units can either ramp down or possibly cycle off, depending on the technology, generation mix, and load characteristics.

1.5 Problem Statement

There is a strong impetus to study the feasibility of increasing renewable energy output in Libya. Integration of PV can reduce overall operating costs for the entire Libyan grid as well as decrease CO_2 emissions. Additionally, international electricity trade is advantageous for Libya due to its location and extent of available solar energy. The steadily decreasing cost of PV modules creates an economic incentive for grid-connected PV systems. Also, operation and maintenance costs of PV are rather low. Generation costs from PV plants will approach that from conventional plants in the near future. Thus, the market for renewable energy will increase faster than conventional fossil fuel power plants. The development of large PV farms in Libya will bring many benefits, such as improving technical capabilities and increasing employment.

This dissertation considers the basic problems associated with the penetration of PV in the Libyan power grid.

1.6 Organization of Dissertation

This study is organized with the purpose of guiding the reader systematically to the work completed in a form with decent readability and overview. Chapter 2 presents

a brief description of the Libyan power system with its past and current state of generation and transmission infrastructure and the potential of solar power plans. Photovoltaic System Fundamentals are discussed in Chapter 3. In chapter 4, a study of the monthly insolation in Libya is presented for a site. Further, it also presents the observed radiation at four locations in Libya to analyze the statistical solar radiation data provided from the solar Electricity Handbook (2017 Edition) using Weibull, Normal, Rayleigh and Gamma distributions. Chapter 5 presents a study of some of the potential impacts of the entry of grid-connected PV on the Libyan power system. Chapter 6 reviews the results of PV integration on the Libyan power system. In particular, the impacts of the penetration of solar power into the electric grid of the city of Al-Kofra with reference to voltage profile are studied. Chapter 7 proposes a methodology for optimal placement of PV plants by selecting candidate buses at which to integrate renewable energy in a distribution system with a high penetration level of solar energy based distributed generations with an objective of enhancing voltage profile. In chapter 8, concluding remarks and future scope are succinctly presented.

CHAPTER 2

LIBYAN ENERGY SCENARIO

Libya is a crude oil exporting nation and the second largest North African country in land with an area of 1,759,540 square km and is located around the Mediterranean Sea with about 1900 km of coastline and 6 million inhabitants. Almost a hundred percent of its territory is land . Libya has virtually no accessible water resources on the earth's surface, consisting of more than 90% of desert or semi-desert [11]. Most prominent natural resources are petroleum and natural gas. These natural resources are the main driving factors for the Libyan economy. It is also due to the abundant fossil resources that Libya has always enjoyed a fairly high international interest and relevance [11]. Libya's economy is dominated by the oil sector, around 95% of export revenues is generated by the energy sector. In terms of solar energy, it could be argued that solar energy is the most important renewable energy resource, as Libya enjoys a high level of insolation. Solar energy is considered to be one of the main resources due to the location of Libya on the cancer orbit line with exposure to the sun‘s rays throughout the year and for long hours during the day.

2.1 Energy Production

In 2012, Libya produced about 30,962 ktoe of energy, which is equivalent to about 34,000 GWh. Clearly, crude oil is by far the most prominent energy source, making up almost 79% of energy production. Another interesting fact is that renewable resources, at least for the year 2011, have been neglected entirely. Recent sources suggest that renewable energy production has only risen to about 0.06% [12] as noted

by the IEA. Figure 2.1 below offers further information on Libya's total energy production trend until 2012.

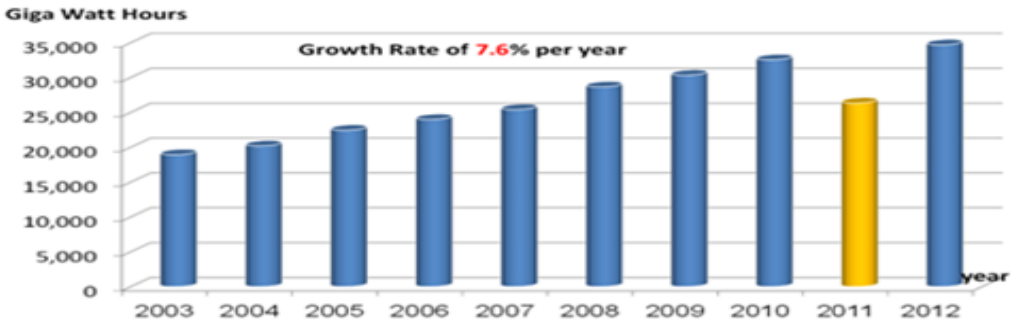

Figure 2.1: Energy production in Libya 2003-2012 [13]

2.2 Energy Consumption

The total amount of energy consumption in Libya was 25,000 GWh in 2011. Commercial sector accounted for 14% whilst the residential sector amounted to 39% and the industrial sector to 17% along with 12% in the agricultural sector. Figure 2.2 shows the energy consumption of Libya in various sectors.

2.3 Electricity Grid

The Libyan national electric grid consists of a high voltage network of about 12,000 km, a medium voltage network of about 12,500 km and 7,000 km of low voltage network. The transmission system comprises of long transmission and subtransmission lines operating at various voltage levels ranging from 400, 220, 132, 66, 30, and 11 KV. Some villages and remote areas, which are located far away from these networks cannot be connected to the grid due to economic reasons. Those locations with a small population and a small amount of energy demand use diesel generators as a power supply, requiring regular maintenance and supply of fuel [14]. There is an operating grid interconnection at 220 kV voltage level to Egypt with a capacity of

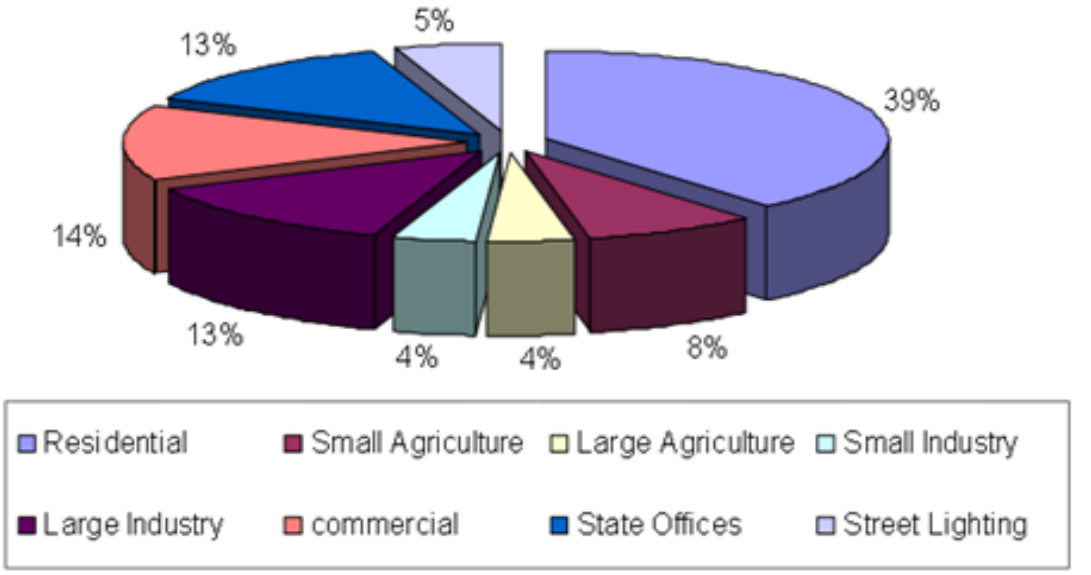

Figure 2.2: The energy consumption in various sectors [13]

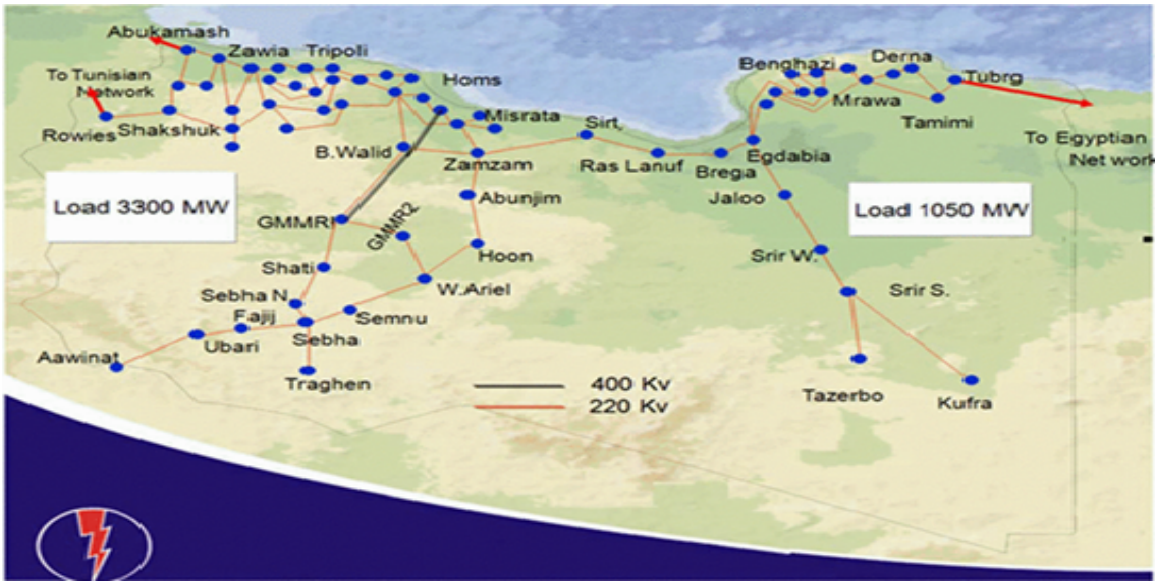

Figure 2.3: Libyan national grid (220 and 400 kV) [16]

240 MW, which is 180 km long and the interconnection between Libya and Tunisia, was completed in 2009 at the 220 kV level [15]. Figure 2.3 shows the Libyan national grid at 220 kV and 400 kV levels.

2.4 Key Problems of the Energy Sector in Libya

There are several aspects of the Libyan energy sector considered to be quite problematic. Due to the abundance of fossil energy sources, renewable energy sources were delegated to secondary relevance. in spite of early efforts of initiating and developing a renewable energy sector under the pre-revolutionary government, the pursuit of a diversified and sustainable energy sector has been limited. Instead of being aggressive on developing alternative energy sources, the old regime strongly subsidized energy obtained from domestic fossil sources. It developed and maintained a fairly one-sided economy that heavily relied and still relies on the availability of fossil fuels. This does not only aggravate future efforts to reform Libya's energy sector, but also dampens the potential advantages of renewable energies and the associated economic and environmental advantages. From a more general point of view, there has been no economic incentive to shift to a more sustainable energy mix.

2.5 Energy Framework

The advantage of utilizing both renewable and traditional energy sources is that the deficiency in one source can be filled by the other one in a normal or controlled mode. Renewable energy cannot be dependable universally due to its stochastic nature. Integration of renewables will decrease the overall reliability of the hybrid system. Integrating conventional sources with renewable sources will result in effective compensation of the weaknesses of renewable sources. In order to reduce its dependence on fossil fuels and to promote renewables, the Renewable Energy Authority of Libya has established targets up to 2030. Long-term plans are to meet 25% of Libya‘s energy supply with renewable energies by the year 2025 and rising to 30% by 2030 [14]. Intermediate targets are 6% by 2015 and 10% by 2020 as shown in Table 2.1.

Table 2.1: Renewable energy share [14]

2015	2020	2025
6% RE Share	**10% RE Share**	**25% RE Share**
750 MW Wind	1500 MW Wind	2000 MW Wind
100 MW CSP	800 MW CSP	1200 MW CSP
50 MW PV	150 MW PV	500 MW PV
150 MW SWH	300 MW SWH	600 MW SWH

2.6 Renewable Energy Sources

Since renewable energy development costs are heavily supported in all economic sectors in Libya, it is difficult to foster renewable energies and energy efficiency on a cost-effective basis. Renewable energies are not utilized in significant amounts and only 5 MW solar energy, in the form of several small PV projects, which have been installed in 2012.

2.6.1 Solar Energy

Suns rays irradiating the earths surface are ultimately the most basic renewable source of energy. Lately, figures supporting the increased use of solar energy for different applications have soared. Libya has significant potential for harnessing solar energy. In the coastal regions, the daily average of solar radiation on a horizontal plane is 7.1 kWh/m2/day and in the southern region, it is 8.1 kWh/m2/day as shown in Figure 2.4 [14]. According to Libyan renewable energy authority, the average duration of sunlight is more than 3,000 hours per year as shown in Figure 2.5. This is equivalent to a layer of 25 cm of crude oil per year on the land surface [14].

2.6.2 Biomass

Libya's biomass potential is limited. Biomass energy sources are small and can only be used on an individual level as an energy source. It is not suitable to produce energy on a large scale.

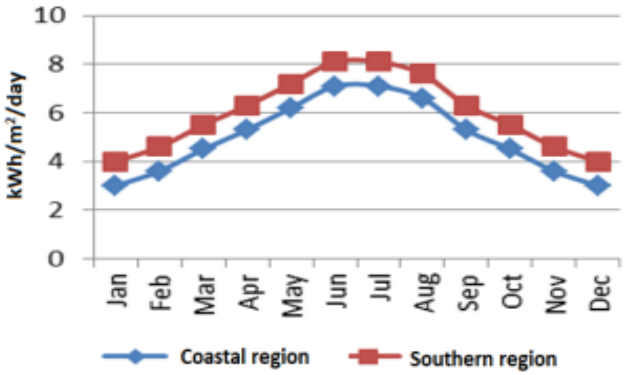

Figure 2.4: The average monthly Daily global radiation in Libya [14]

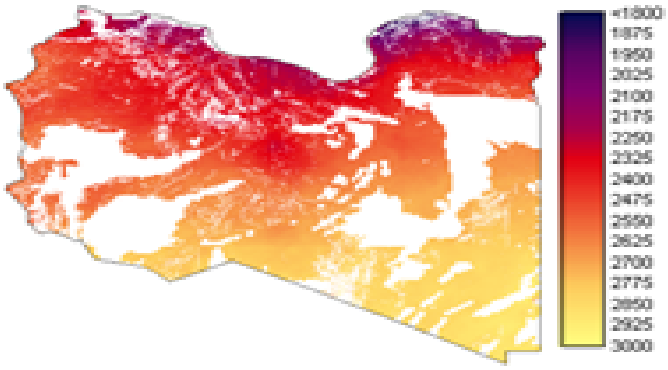

Figure 2.5: The average global radiation on the horizontal plane [17]

2.6.3 Wind Energy

Wind energy in Libya was exploited to pump water during the mid- 20th century. Modern interests in wind power exploitation have only recently reemerged [15]. Since the wind-mills need to be maintained regularly, this way of producing energy has not been developed on a large scale. Libyan authorities have recognized the importance of seeking alternative sources of power as well as integrating wind power into electricity networks. The wind potential is good and the average wind speed at 40-meter height is between 6-7.5 m/s [12]. One of the several attractive locations along the Libyan coast is at Dernah where the average wind speed is around 7.5-8 meters per second as shown in Figure 2.6.

In 2000, the General Electric Company of Libya (GECOL), in collaboration with the Center for Solar Energy Studies (CSES), started to take some steps to study

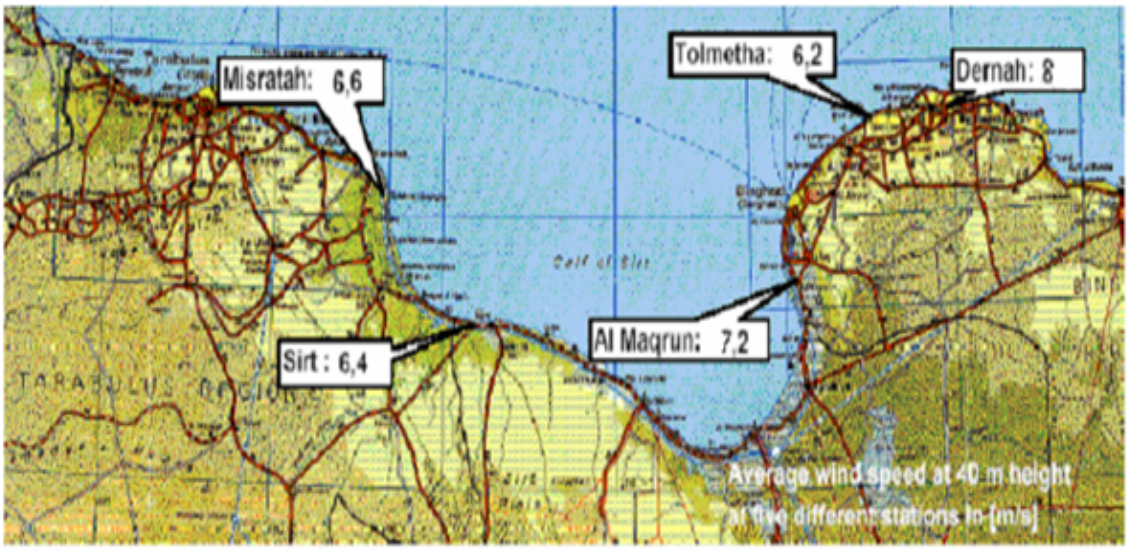

Figure 2.6: Average wind speed measured in different locations in Libya [18]

and develop small scale wind power applications. They began to seek specialists in wind energy technology to evaluate the potential of harnessing the energy in wind for generating electricity in Libya.

CHAPTER 3

PHOTOVOLTAIC SYSTEM FUNDAMENTALS

One way of utilizing the energy of the sun is to generate electricity directly from sunlight by employing photovoltaic (solar cells) systems. The photovoltaic effects is defined as the generation low-voltage dc output by the absorption of incident photons [19]. Groups of PV cells are electrically configured into modules and arrays, the output of which is used to charge batteries, operate motors, and to power any number of electrical loads. With appropriate power conversion equipment, PV can provide alternating current supply compatible with any conventional appliance and can also operate in parallel with the utility grid.

3.1 History of Photovoltaics

The first PV cells produced in the late 1950s and throughout the 1960s were principally used to provide electrical power for earth-orbiting satellites. In the 1970s, improvements in manufacturing, performance, and quality of PV modules helped to reduce costs and opened up a number of opportunities for powering remote terrestrial applications, including battery charging for navigational aids, signals, telecommunications equipment and low power needs. In the 1980s, PV became a popular power source for consumer electronic devices, including calculators, watches, radios, lanterns and other small battery charging applications. Following the energy crisis of the 1970s, significant efforts resulted in the development of PV power systems for residential and commercial uses both for stand-alone, remote power as well as for utility-connected applications. During the same period, global applications for PV to power remote

rural health clinics, refrigerators, water pumping, telecommunications, and off-grid households increased dramatically, and continues to be a significant portion of the present world market for PV products [20].

3.2 Principles of PV- Device Operation

PV devices are made of semiconductor materials in the form of p-n junctions that can generate electricity by the absorption of incident photons. Minority carriers generated by the absorption of photons in the semiconductor material (holes in n-region, and electrons in p-region) diffuse and reach the junction region in which there is an internal electric field, which separates the electrons and holes. Electrons accelerate into the n-region and the holes into the p-region. This causes the n-region to accumulate a negative charge and the p-region builds up a positive charge, resulting in a photo-voltage. If there is a closed external path, a photocurrent results and the associated photo-voltage appears across the external load resistance as illustrated in Figure 3.1. Atoms with one more valence electron than silicon are used to produce n-type semiconductor materials. Atoms with one less valence electron result in p-type material. This process of adding impurities is called doping. Once the n-type and p-type semiconductor materials are formed into a p-n junction, an output voltage results with the absorption of incident photons. The most common doping materials used in forming n-type and p-type semiconductor materials are phosphorus and boron [21]. A p-n junction can be formed either by a high-temperature diffusion process or an ion implantation process. Diffusion can be made from either a vapor phase or a solid phase. Crystalline silicon and amorphous silicon are the most dominant semiconductor materials for commercial PV cells [21].

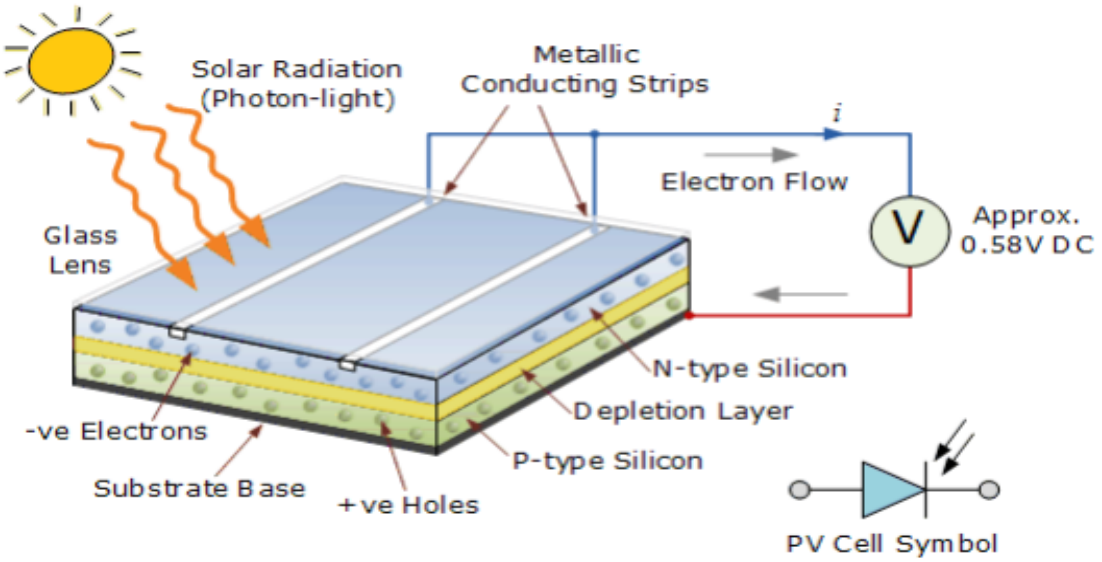

Figure 3.1: PV cell operation diagram [21]

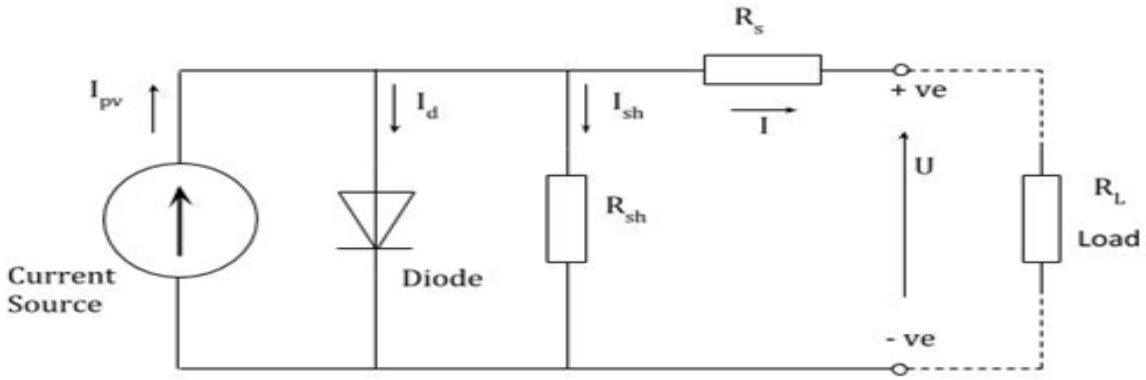

Figure 3.2: Equivalent circuit of a solar cell including a resistive, load [22]

3.2.1 Equivalent Circuit of a Solar Cell

The equivalent circuit of a solar cell consists of a current source I_{pv}, a nonlinear device (diode) in parallel a shunt resistance R_{sh} to account for leakage near the edge and corner of the cell, a series resistance R_s due to the resistance of the bulk cell material and the resistance encountered when charge carriers travel along the thin top sheet of n- or p-type doped material, the contact resistance, and finally a resistive load R_L [22]. Figure 3.2 shows the equivalent circuit.

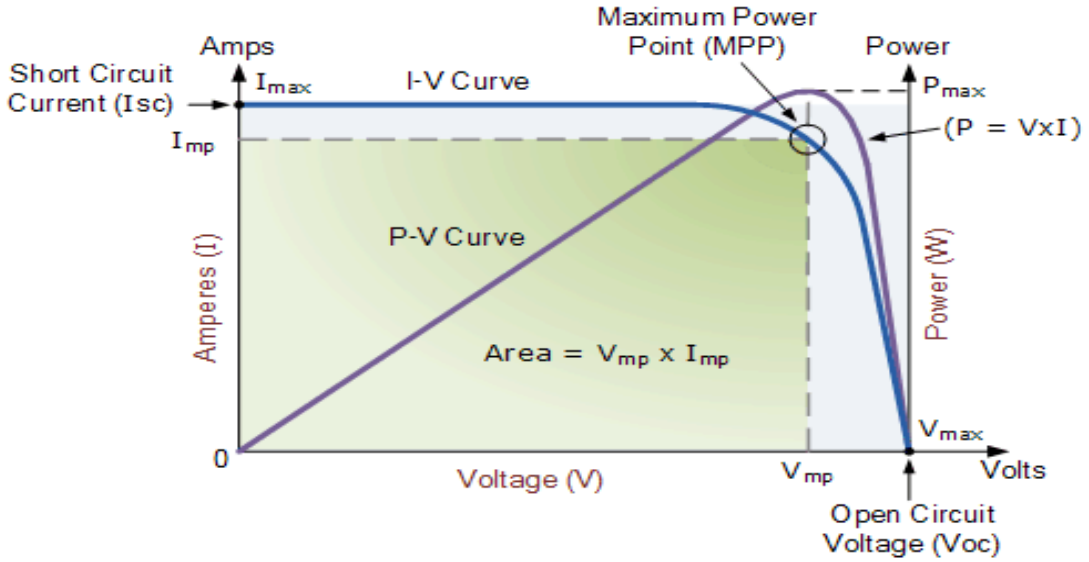

Figure 3.3: Current-voltage characteristic with the power curve of solar cell [21]

3.2.2 Current Voltage Characteristic

Solar cell I-V characteristics curves are shown in Figure 3.3. They are basically graphical representations of the operation of a solar cell or module summarizing the relationship between output current and voltage under existing conditions of irradiance and temperature. I-V curves provide the information required to configure a solar system so that it can operate as close to its optimal peak power point (MPP) as possible. With the solar cell under open circuit condition, the current will be at its minimum (zero) and the voltage across the cell is at its maximum, known as open circuit voltage (V_{oc}). On the other hand, when the solar cell is short circuited, that is the positive and negative leads connected together, the voltage across the cell is at its minimum (zero) but the current output of the cell reaches its maximum, known as short circuit (or source) current (I_{sc}). The maximum voltage available from a cell is at open circuit, and the maximum current at short circuit. There is one particular combination of current and voltage for which the output power reaches its maximum value, at I_{mp} and V_{mp}. Therefore ideal operation of a photovoltaic cell is defined to be at the maximum power point (MPP).

3.2.3 Efficiency and Fill Factor

The efficiency is defined as the ratio of energy output from the solar cell to input energy from the sun incident on the cell area. In addition to reflecting the performance of the solar cell itself, efficiency depends on the spectrum and intensity of the incident sunlight and the temperature of the solar cell.

The efficiency of a solar cell is determined as the fraction of incident power, which is converted to electricity and is defined as:

$$\eta = \frac{P_{out}}{P_{in}} \tag{3.1}$$

$$= \frac{P_{out}}{P_s.A_s} \tag{3.2}$$

where:

P_{out} the electrical output power of the cell.

P_{in} The input power of the cell.

P_s The solar radiation level per unit area.

A_s The active cell area.

The maximum cell efficiency can be defined as:

$$\eta_{max} = \frac{I_{mp.V_mp}}{P_{in}} \tag{3.3}$$

where:

I_{mp} Current at maximum power point.

V_{mp} Voltage at maximum power point.

The maximum voltage and current achievable are V_{oc} and I_{sc}.

The fill factor (FF) is defined as the ratio of the maximum power from the solar

cell to the product of V_{oc} and I_{sc}.

$$FF = \frac{I_{mp.V_{mp}}}{I_{sc.V_{oc}}} \tag{3.4}$$

A larger fill factor is desirable, and corresponds to an I-V characteristic that is more rectangular. Typical fill factors range from 0.5 to 0.82. Fill factor is also often represented as a percentage.

3.3 Incident Solar Irradiation (Insolation)

The solar radiation incident on PV depends critically on the location and the spectral distribution of the radiation coming from the sun [23]. To a good approximation, the sun acts as a perfect emitter of radiation (black body) at a temperature close to 5800 K. In general, the total power from a radiant source falling on a unit area is called irradiance [21].

3.3.1 Calculation of Average Power for One PV Module

The electrical power generation and the terminal voltage of PV module depends on solar irradiance and ambient temperature. The circuit model consists of a light-dependent current source and a group of resistances, including internal shunt resistance, R_{sh}, and series resistance, R_s as shown in Figure 3.2. The series resistance should be as low as possible, but the shunt resistance should be very high, so that most of the available current can be delivered to the load. The mathematical equation describing the I-V characteristics of a PV solar cells module are given by [24]:

$$I(t) = I_{ph}(t) - I_o(t) * \left(exp\left(\frac{q * (V(t) + I(t) * R_s)}{A * KB * T(t)} \right) - 1 \right) - \frac{(V(t) + I(t) * R_s)}{R_{sh}} \tag{3.5}$$

where:

$I(t)$ The output current at time t, Amp.

$V(t)$ The output voltage at time t, Volt.

I_{ph} current generated by PV, A.

I_o reverse saturation current, V.

A The ideality factor for p-n junction.

$T(t)$ The temperature at time t, Kelvin.

KB The Boltzman's constant in Joules per Kelvin, $1.38 * 10^{-23} J/k$

q The charge of the electron in Coulombs, $1.6 * 10^{-19} C$.

$I_O(t)$ The reverse saturation current at time t, Amp.

This current varies with temperature as follows [24]:

$$I_o(t) = I_{or}(t) * \Big(T(t)/T_r\Big)^3 * exp\left[\frac{q * E_{go}}{KB * A\Big(1/T_r - 1/T(t)\Big)}\right] \tag{3.6}$$

$I_{ph}(t)$ The generated current at time t of solar cells module. which is given by [24]:

$$I_{ph}(t) = (I_{sc} + K_I(T(t) - 298)) * H_T(t)/100 \tag{3.7}$$

where:

T_r The reference temperature, oK.

E_{go} The band-gap energy of the semiconductor used in solar cells module.

K_I The short circuit current temperature coefficient.

I_{or} The saturation current at Tr, Amp.

$H_T(t)$ The average hourly radiation on the tilted surface, kW/m^2.

Isc PV cell short-circuit current at $250°C$ and $100mW/cm^2$.

The output of the solar cells module at time t can be calculated by the following equation [25]:

$$P_{pv,out}(t) = V(t) * \left[I_{ph}(t) - I_o(t) * \left(exp\left(\frac{q * (V(t) + I(t) * R_s)}{A * KB * T(t)} \right) - 1 \right) - \frac{(V(t) + I(t) * R_s)}{R_{sh}} \right] \tag{3.8}$$

From the above equations, it can be concluded that the output current and power of a PV module are affected by insolation and the operating of cell temperature.

3.4 PV Cells, Modules and Arrays

PV cells are connected in series and parallel to produce the required voltage and current levels from a PV module. The inter-connection of modules on a support structure is called a PV array as shown in Figure 3.4.

PV modules represent the basic building block of a PV generator. The modules are connected in series to form strings where the number of series modules is determined by the required DC bus voltage and the number of parallel strings depends on the required load current [21].

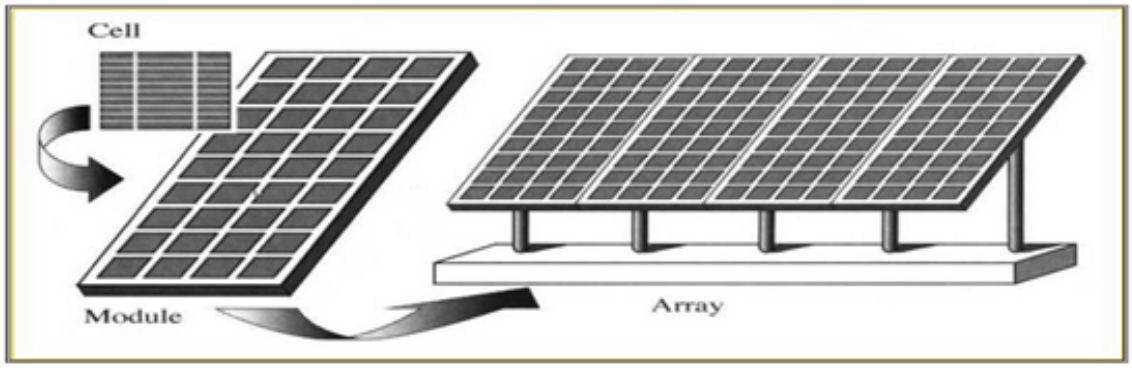

Figure 3.4: PV Cells, Modules and Arrays [21]

3.5 Balance of System Equipment

In addition to the PV modules, there is a balance-of-system (BOS) equipment needed to operate the PVs. This includes battery charge controllers, batteries, inverters (for loads requiring alternating current), wires, conduit, earthing, fuses, safety disconnects, outlets, metal structures for supporting the modules, and any additional components that are part of the PV system [26].

3.5.1 Charge Controller

The charge controller regulates the flow of electricity from the PV modules to the battery as well as to the connected load. The controller keeps the battery fully charged without overcharging it. When the controller senses that the battery is fully charged, it stops the flow of charge from the modules to the battery. Typically controller also senses when the batteries are overloaded, and automatically disconnects parts of the load until sufficient charge is restored to the batteries. This last feature can greatly extend the battery's lifetime. Charge controller costs generally depend on the ampere capacity at which PVs will operate and the monitoring features required [27].

3.5.2 Battery

The battery stores electricity for use at night or for meeting load demands during the day when the modules are not generating sufficient power to meet load requirements. To provide electricity over long periods, PVs require deep-cycle batteries. These batteries are designed to gradually discharge and recharge up to 80% of their capacity hundreds of times. Automotive batteries are shallow-cycle batteries and should not be used in PVs because they are designed to discharge only about 20% of their capacity, the climatic conditions in which it will operate, how frequently it will receive maintenance, and the types of chemicals it uses to store and release electricity. PV system may have to be sized to store a sufficient amount of energy in the batteries

to meet power demand during several days of cloudy weather, also known as days of autonomy [26][28].

3.5.3 Inverter

To power AC equipment inverter is required, which converts the DC electricity produced by PV modules and stored in batteries into AC electricity. Different types of inverters produce different qualities of electricity. For example, lights, television, and power tools can operate on lower-quality electricity, but computers, laser printers, and other sophisticated electronic equipment require the highest-quality electricity. So, matching the power quality required by the loads with the power quality produced by the inverter is important [27].

Inverters cost for most stand-alone applications is affected by several factors, including the quality of the electricity needed to produce and whether the incoming DC voltage is 12, 24, 36, or 48 volts. The AC power required, the amount of extra surge power and the AC loads need for short periods, whether the inverter has any additional features such as meters and indicator lights [28].

3.6 Types of PVs

PV systems are generally classified according to their functional and operational requirements and how the equipment is connected to other power sources and electrical loads. The two principal classifications are either stand alone or grid connected system [21].

3.6.1 Stand Alone PVs

PVs are designed to operate independent of the electric utility grid in its simple form. It consists of the array supplying the load directly, as shown in Figure 3.5, used for battery charging via charge controller or for water pumping, where the storage

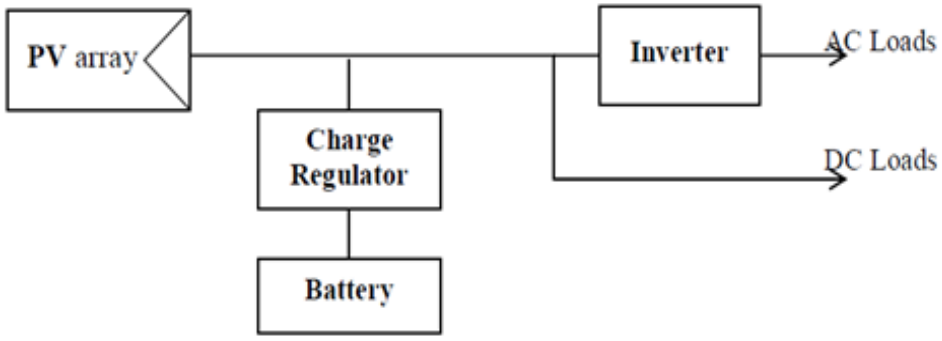

Figure 3.5: Stand-alone AC/DC system with battery storage

medium is a storage tank.

3.6.2 Grid-Connected PVs

Schematic of grid-connected PV is shown in Figure 3.6. They are designed to operate in parallel and interconnected with the electric utility grid. The primary component in grid-connected PVs is the inverter. The inverter converts the DC power produced by the PV array into AC power consistent with the voltage and power quality requirements of the utility grid, and automatically stop supplying power to the grid when the utility grid is not energized. This allows the AC power produced by the PVs either to supply on-site electrical loads or to back feed the grid when the PVs output is greater than the on-site load demand. At night and during other periods when the electrical loads are greater than the PVs output, the balance of power required by the loads is supplied by the electric utility. The above schematic can be varied to suit particular applications. For example, the PV array may be divided into sub arrays each with its own inverters to improve the system performance.

3.7 Advantages and Disadvantages of PVs

The advantages that photovoltaic systems have over competing power options are:

1. There is no fuel supply problem (free fuel)

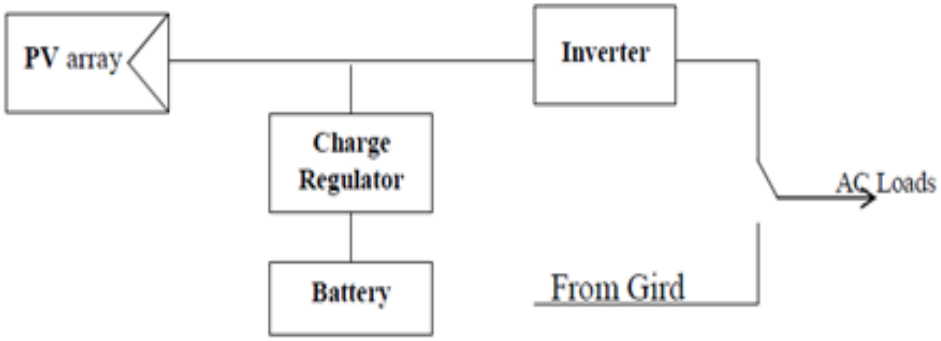

Figure 3.6: Grid Connected PVs

2. Long lifetime (over 20 years)

3. Pollution free

4. High reliability

5. Require very little maintenance

6. Easy to install

7. Easy to expand

These advantages make them suitable for remote or isolated locations. The PVs have a few disadvantages as well, they are:

1. Initial cost is high.

2. Conversion efficiency is low

3.8 PVs Market Overview

In 2004 more than 2700 MWp of PV were installed worldwide and its applications share is as shown in Figure 3.7. China has the highest installed capacity followed by Japan, Germany and USA. These four countries represent about two third global PV capacity. Market growth rate in the last 10 years has been between 20% and 40% per

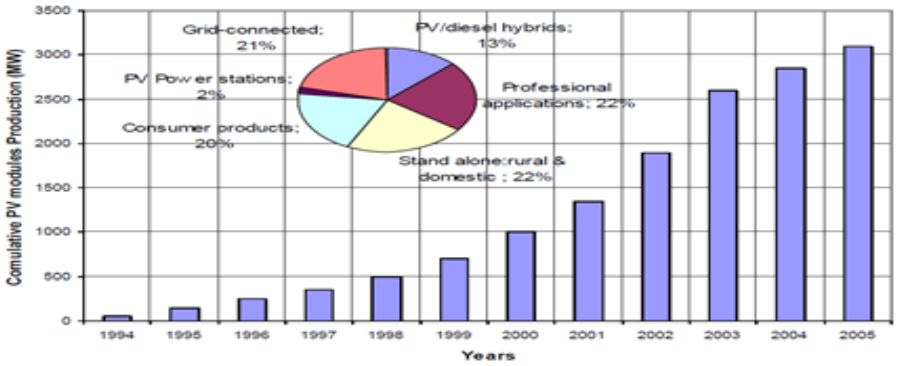

Figure 3.7: World PV modules production, consumer and commercial (MW) [29]

year. In recent decades, there was a price reduction of 20%, every time the market volume doubled. As a result, of this, photovoltaic prices dropped by about 50% every decade. It is not sure how long this price reduction process will continue. However, PVs have the potential to become competitive even with conventional grid-connected systems in a few decades [29].

The cost of a PV module is measured in dollars per peak-watt \$/Wp, where "peak watt" is defined as the power under full sunlight at sea level on a clear day. Modules are rated using standard test conditions, which is 1000 W/m^2, an air mass of 1.5 at 25°C. Thus, PV module "cost reduction" is the result of either a decrease in manufacturing cost or an improvement in module efficiency. Cost of crystalline silicon PV module process has decreased from \$51/Wp to approximately \$3.50/Wp by 2002 [29].

CHAPTER 4

A STUDY OF THE MONTHLY INSOLATION IN LIBYA

Solar energy is highly site specific and readily available. Solar technologies are pollution free and therefore act as the leading potential source of alternative energy. Moreover, cost of photovoltaic (PV) modules has been declining significantly at an average rate of 20% with each doubling of sales. The knowledge of available solar radiation of a location is a fundamental requirement before embarking on any solar energy project such as photovoltaics farm, solar thermal system, and passive solar design [67]. Many developing countries do not have the equipment for continuous and exact measurements of solar radiation because of expensive measuring facilities and techniques required. It is therefore, necessary to develop alternative methods to estimate the solar radiation of potential locations. Knowing the probability distribution function of any time series data such as solar radiation of a site enables someone to generate data that will have the same characteristic as the actual data for any solar power project. In this chapter, probability distribution functions that best model the solar radiation data of the four cities (Hoon, Al-Quryat, Jalo, Al-Kofra) of Libya are obtained based on goodness of fit tests, similar to the application of statistical analysis of solar radiation data in Taiwan [31].

Incident Solar radiation (insolation) is a renewable energy source and its use has accelerated around the world. It is stochastic in nature and the insolation at a location varies randomly with time. Understanding the statistical properties of solar irradiation is essential for predicting the energy output of a solar energy conversion system. A proper analysis of insolation data is a very important step, not only for

Table 4.1: The information of the meteorological stations

Station	Latitude °N	Longitude °E
Hoon	29 02	16 00
Al-Quryat	31 19	20 03
Jalo	24 17	23 15
Al-Kofra	29 42	24 38

structural and environmental design and analysis but also for the assessment of the solar energy potential [32]. The purpose of this study is to find the most appropriate distributions for describing solar radiation in Libya. Suitability of Weibull, Normal, Gamma, and Rayleigh distribution are compared by using different goodness of fit criteria. Furthermore, Root Mean Square Error (RMSE) and correlation coefficient (R) are also used to compare distributions to assess their suitability. In terms of solar energy, it could be argued that it is the most important renewable energy resource, as Libya enjoys a high-level of insolation. Four locations in Libya are considered and the geographic details of the locations are summarized in Table 4.1.

4.1 Monthly Insolation Data

Modeling radiation by statistical analysis in terms of distribution functions has been well documented in this study. Although several probability distribution functions have been used, the best four among them are reported in this chapter. Concepts such as the goodness of fit tests, root mean squared error (RMSE) and the correlation coefficient (R) were applied to find the best fit probability distributions. The analysis was conducted on monthly solar radiation data to gain insight of the data. Solar radiation data at four locations used in this study are obtained from the Solar Electricity Hand Book (2017 Edition) as presented in Table 4.2 [33]. The inability of the electricity utility company to meet the required electricity demand and the availability of good solar radiation throughout the year makes those cities of Libya good candidates for various solar power projects.

Table 4.2: Average monthly solar radiation ($kWh/m^2/day$) [33]

Month	Hoon	Al-Quryat	Jalo	Al-Kofra
Jan	3.93	3.67	3.63	3.50
Feb	4.92	4.57	4.89	4.56
Mar	5.75	5.13	5.66	5.60
Apr	6.40	5.95	6.08	6.52
May	6.73	6.49	6.45	6.92
Jun	7.16	7.25	7.14	7.38
Jul	7.40	7.14	6.97	7.51
Aug	7.00	6.78	6.67	7.20
Sep	6.14	5.67	5.93	6.49
Oct	5.29	4.66	5.24	5.42
Nov	4.08	3.56	3.81	4.05
Dec	3.67	3.35	3.25	3.37
Year Avg	5.70	5.35	5.47	5.71
Year S.D	1.31	1.40	1.33	1.52

4.2 Probabilistic Model For Solar Radiation Data

Insolation is stochastic and it can be modeled are a random variable in a particular area by a suitable probability distribution function. We need to identify the distribution, which is the best fit of data. The cumulative distribution function $F(x)$ of the irradiation x gives the probability that the solar irradiation is equal to or less than x. Several distributions for solar irradiation are discussed, as a means to represent the nature of insolation.

4.2.1 A. Weibull Distribution

The Weibull probability density function has been widely used, accepted and recommended to model solar irradiation and to estimate solar energy potential [34, 35]. The general form of the Weibull density function for solar irradiation is given by Equation 4.1:

$$f(x) = \left(\frac{\alpha}{\beta}\right)\left(\frac{x}{\alpha}\right)^{\beta-1} exp\Big[-\left(\frac{x}{\alpha}\right)^{\beta}\Big] \tag{4.1}$$

In Equation 4.1 $f(x)$ is the probability density function of the random variable solar irradiation x. β is the dimensionless shape parameter and α is the scale parameter having units of solar radiation ($kWh/m^2/day$). The corresponding cumulative distribution function is given in Equation 4.2:

$$F(x) = 1 - exp\Big[- \left(\frac{x}{\alpha}\right)^{\beta} \Big] \tag{4.2}$$

There are several methods to estimate Weibull parameters as summarized in [36, 37]. Values of α and β can be obtained by the method of moments, maximum likelihood, Weibull probability paper (graphic method) and power density. The moment method using the mean solar radiation μ and standard deviation σ is employed in this study. The applicable equations are given by 4.3 to 4.6:

$$\mu = \alpha\Gamma\Big(1 + \frac{1}{\beta}\Big) \tag{4.3}$$

$$\left(\frac{\alpha}{\mu}\right)^2 = \left[\frac{\Gamma\Big(1 + \frac{2}{\beta}\Big)}{\Gamma^2\Big(1 + \frac{1}{\beta}\Big)}\right] - 1 \tag{4.4}$$

$$\beta = \left(\frac{\alpha}{\mu}\right)^{-1.086} \tag{4.5}$$

$$\alpha = \frac{\mu}{\Gamma\Big(1 + \frac{2}{\beta}\Big)} \tag{4.6}$$

4.2.2 B. Normal Distribution

The probability density function for normal distribution and the cumulative distribution function are given by [35]:

$$f(x) = \frac{1}{\sigma\sqrt{2\pi}} exp\Big[- \Big(\frac{x - \mu}{2\sigma^2}\Big)^2 \Big] \tag{4.7}$$

$$F(x) = \frac{1}{2}\Big[1 + erf\Big(\frac{x-\mu}{\sigma\sqrt{2}}\Big)\Big] \tag{4.8}$$

Where μ and σ are the mean and standard deviation of the solar radiation x and the erf ( ) is the error function given by:

$$erf(x) = \frac{2}{\sqrt{\pi}}\int_0^x exp(-t^2)dt \tag{4.9}$$

4.2.3 C. Gamma Distribution

The gamma distribution is a two parameter distribution that has properties similar to those of the Weibull distribution. The two parameters, a scale parameter α and shape parameter β, can be adjusted to fit observed data [35]. The probability density function of gamma distribution is given as:

$$f(x) = \frac{x^{\beta-1}}{\alpha^{\beta}\Gamma(\beta)}exp\Big[-\Big(\frac{x}{\alpha}\Big)\Big] \tag{4.10}$$

Where x is the measured solar radiation data. The cumulative distribution function is given by:

$$F(x) = \frac{1}{\alpha^{\beta}\Gamma(\beta)}\int_0^x t^{\beta-1}exp\Big[-\Big(\frac{t}{\alpha}\Big)\Big]dt \tag{4.11}$$

4.2.4 D. Rayleigh Distribution

Rayleigh distribution can be considered as a special case of Weibull distribution by setting β as 2, [38]. By setting $\beta = 2$, evaluating and rearranging the expression in (4.1), the probability density function of Rayleigh is given as:

$$f(x) = \frac{x}{\alpha^2}exp^{-\frac{x^2}{2\alpha^2}} \tag{4.12}$$

Where α is given as

$$\alpha = \sqrt{\frac{2}{\pi}}\mu \tag{4.13}$$

Similarly, the cumulative distribution function F(x) of Rayleigh distribution is given as,

$$F(x) = 1 - exp^{-\frac{x^2}{2\alpha^2}} \tag{4.14}$$

4.3 Goodness of Fit Tests

The Goodness of fit test is a statistical test that determines whether a particular distribution fits the data on hand. In this study, two goodness of fit tests were applied at 5% level of significance to check how accurate the distribution model fits the observed data. They are Chi-Squared test χ^2, and Kolmogorov-Smirnov test KS. Root mean square error (RMSE) and correlation coefficient (R) are also used to determine the error and assess the correlation between data series and each distribution. The distribution, which results in the highest value for R, and the lowest value for RMSE, is the most accurate model fit for the observed data.

4.3.1 Chi-Squared Test

This test is used to determine whether the sample data set fits a specified distribution [39]:

$$\chi^2 = \sum\nolimits_{i=1}^{k} \frac{\left(O_i - E_i\right)^2}{E_i} \tag{4.15}$$

Where O_i denotes the observed frequency and E_i denotes the expected frequency.E_i, calculated using [37]:

$$E_i = n\int_{xL}^{xU} f(x) = n\Big[F(x_U) - F(x_L)\Big] \tag{4.16}$$

Where $f(x)$ is the specified probability density function, $F(x)$ is the corresponding

Table 4.3: Test statistic values of Chi-Squared test

Locations	Chi-squared test				
	C.V	Weibull	Rayleigh	Normal	Gamma
Hoon	9.48	2.813	5.583	3.530	4.415
Al-Quryat	9.48	2.537	3.650	2.738	2.584
Jalo	9.48	4.008	8.068	4.429	4.827
Al-Kofra	9.48	1.896	5.581	2.388	3.209

cumulative distribution, and x_U, x_L are the lower and upper limits of the i^{th} bin.Value of test statistic χ^2 must be less than critical value C.V to be considered that the sample data set follows a specified distribution as shown in Table 4.3.

4.3.2 Kolmogorov-Smirnov Test

The Kolmogorov-Smirnov KS test is based on the largest difference between the observed cumulative distribution function $F_o[x_{(i)}]$ and hypothesized cumulative distribution function $F_T[x_{(i)}]$. A value of test statistic d given as [40].

$$d = max_{i=1}^{n}\Big(|F_O[x_i] - F_T[x_i]|\Big) \tag{4.17}$$

where

$F_O[x_i] = \dfrac{i}{n}$

For $i = 1, 2, ...n$

Similarly, the value of test statistic d must be less than the critical value to be considered that the sample data set follows a specified distribution as shown in Table 4.4.

Table 4.4: Test statistic values of Kolmogorov-Sminrov test

Location	Kolmogorov-Smirnov				
	C.V	Weibull	Rayleigh	Normal	Gamma
Hoon	0.37	0.320	0.722	0.317	0.430
Alquriat	0.37	0.175	0.735	0.160	0.308
Jalo	0.37	0.156	0.759	0.285	0.363
Al-Kofra	0.37	0.296	0.760	0.221	0.374

4.4 Root Mean Square Error

Root mean square error (RMSE) is a parameter used to assess how closely a model fits some data. It is a tool used to inspect the quality of the fit. The RMSE can be estimated by following expression [41].

$$RMSE = \sqrt{\frac{1}{k}\sum_{i=1}^{k}\left(O_i - E_i\right)^2} \tag{4.18}$$

High RMSE values can indicate problems, and the smaller the RMSE, the closer model follows data. Corresponding results are also presented in Table 4.5.

4.4.1 Correlation Coefficient

The correlation coefficient (R) describes the correlation between the data series, where the value of R ranges between -1, a perfect negative correlation, and $+1$, a perfect positive correlation. The correlation coefficient is given by [41].

$$R = \frac{1}{k-1}\sum_{i=1}^{k}\frac{(O_i - O_m)(E_i - E_m)}{\sigma_O \sigma_E} \tag{4.19}$$

Where O_m , E_m denote the means of observed frequency and expected frequency respectively. σ_O, σ_E are the standard deviation of observed frequency and expected frequency respectively. Results of correlation coefficient are presented in Table 4.6 for the four sites under study.

Table 4.5: Test statistic values of Root Mean Square Error

Location	RMSE			
	Weibull	Rayleigh	Normal	Gamma
Hoon	0.977	1.173	1.086	1.210
Al-Quryat	0.878	1.030	0.909	0.9271
Jalo	1.178	1.519	1.280	1.441
Al-Kofra	0.808	1.173	0.901	1.043

Table 4.6: Test statistic values of Correlation Coefficient

Location	R			
	Weibull	Rayleigh	Normal	Gamma
Hoon	-0.21	0.06	-0.16	0.0007
Al-Quryate	-0.58	-0.25	-0.58	0.0010
Jalo	-0.12	0.05	-0.16	-0.3493
Al-Kofra	-0.25	-0.89	-0.34	-0.3587

4.5 Simulation Results

Some standard continuous probability distributions were carefully chosen based on their shape parameters to fit the data, also parameter values for each probability distribution are determined by using the corresponding mean and standard deviations of solar radiation, calculated from available data of the overall and individual twelve months for four locations in Libya. As mentioned, for the whole year, the average solar radiation is $5.70 kWh/m^2/day$ for the city of Hoon, $5.43 kWh/m^2/day$ for the city of Al-Quryat, $5.47 kWh/m^2/day$ for the city of Jalo and $5.71 kWh/m^2/day$ for the city of Al-Kofra. The solar radiation for the individual month has the maximum monthly mean value between 7.14 to $7.51 kWh/m^2/day$, which occurs in June and July while a minimum value between 3.2 to $3.93 kWh/m^2/day$ occurs in December and January. Weibull, Normal, Gamma and Rayleigh are fitted to solar radiation data. Parameters of these distributions are estimated analytically based on actual data by using formulas described in the previous section. The results are presented in Table 4.7.

Two goodness of fit tests were used to identify the best fit at 5% level of signifi-

Table 4.7: Parameters in distribution in four locations in Libya

Location	Weibull		Rayleigh	Normal		Gamma	
	α	β	α	μ	σ	α	β
Hoon	5.8	4.1	4.2	5.3	1.4	13.9	0.3
Al-Quryat	6.0	3.8	4.3	5.4	1.5	12.1	0.4
Jalo	6.0	4.4	4.3	5.4	1.3	15.3	0.3
Al-Kofra	6.3	4.2	4.6	5.7	1.5	14.3	0.4

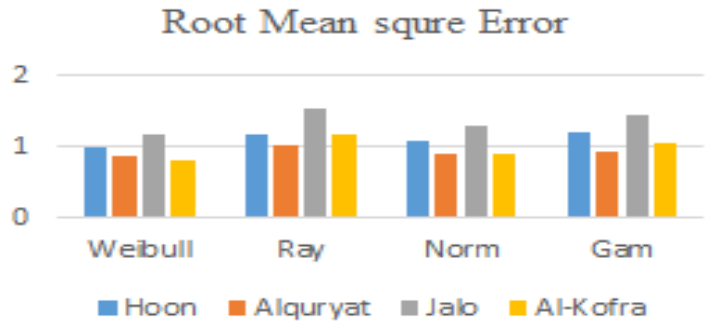

Figure 4.1: Root mean square error for each distribution and location

cance. They are Chi-Squared test, and Kolmogorov-Smirnov test. The test statistic values for these tests are presented versus critical values of each test in Tables 4.3 and 4.4. According to χ^2 test it is observed that all cities have test statistic less than critical value for all distributions and for KS test it is observed that all cities have test statistic less than critical value for all distributions. Root mean square error (RMSE) and correlation coefficient (R) values were also used to determine both the error and the correlation and these values are presented in Table 4.5 and 4.6. It is observed that for Weibull and Normal distributions, the largest values of RMSE are the lowest and the largest values of R are the highest. Root mean square error (RMSE) and correlation coefficient (R) of each distribution is plotted for individual cities, as shown in Figure 4.1 and Figure 4.2.

Weibull, Normal, Rayleigh and Gamma distributions are plotted along with the

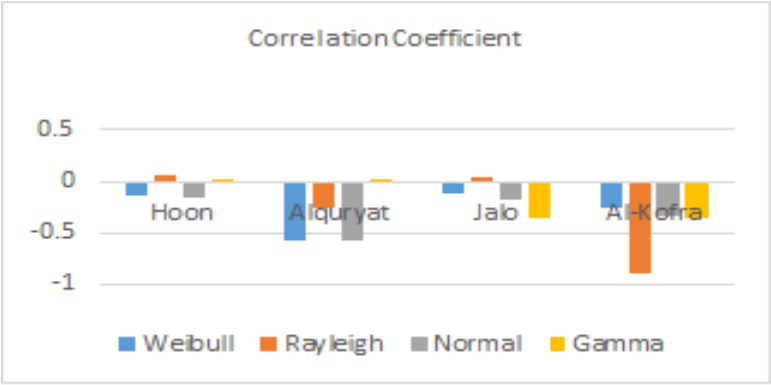

Figure 4.2: Correlation coefficient for each distribution and location

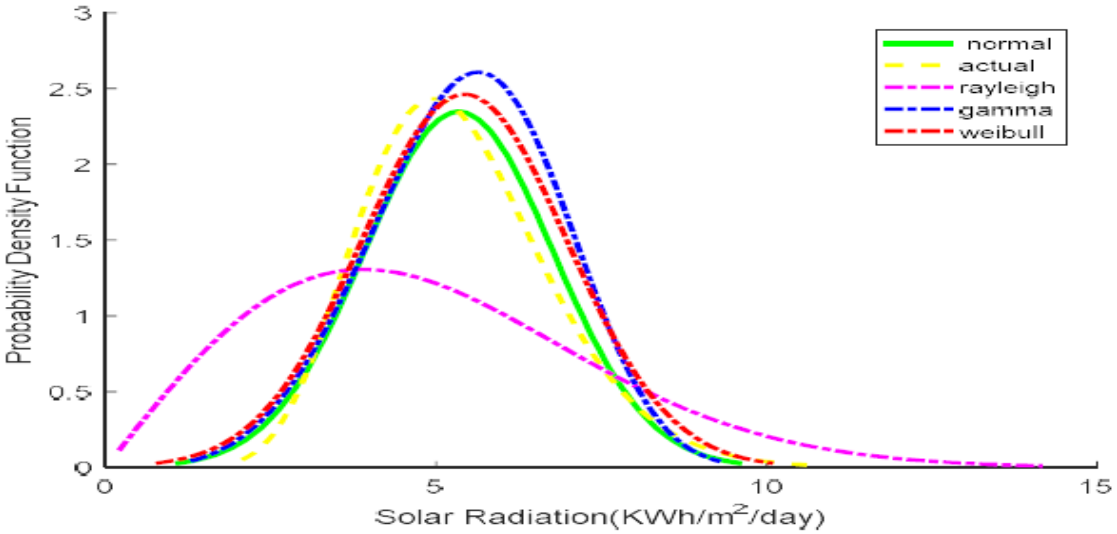

Figure 4.3: Fitting pdf to the actual data of Hoon

actual probability density function of solar radiation for each city in Figures 4.3 through 4.6.

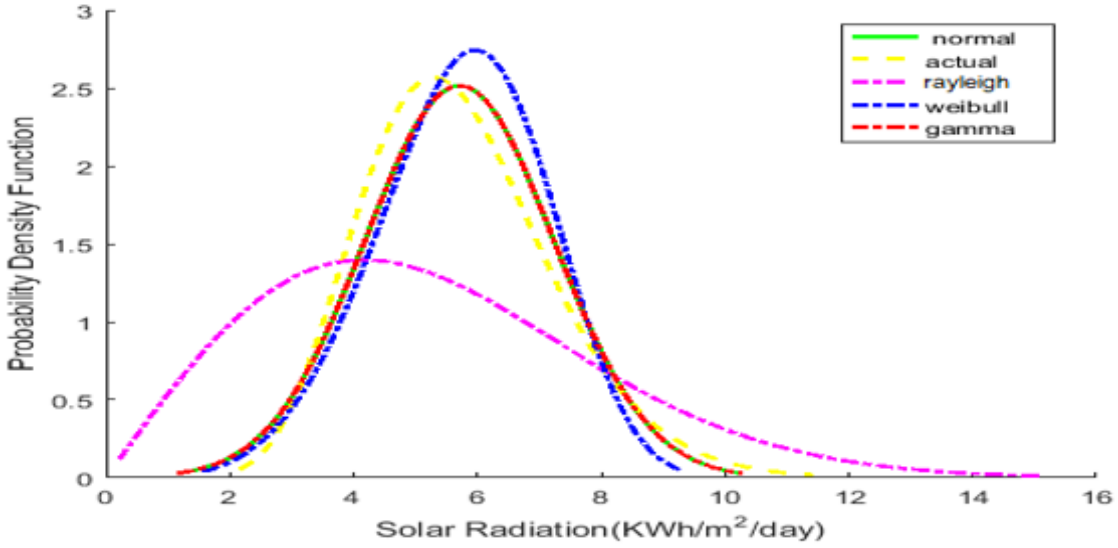

Figure 4.4: Fitting pdf to the actual data of Al-Quryat

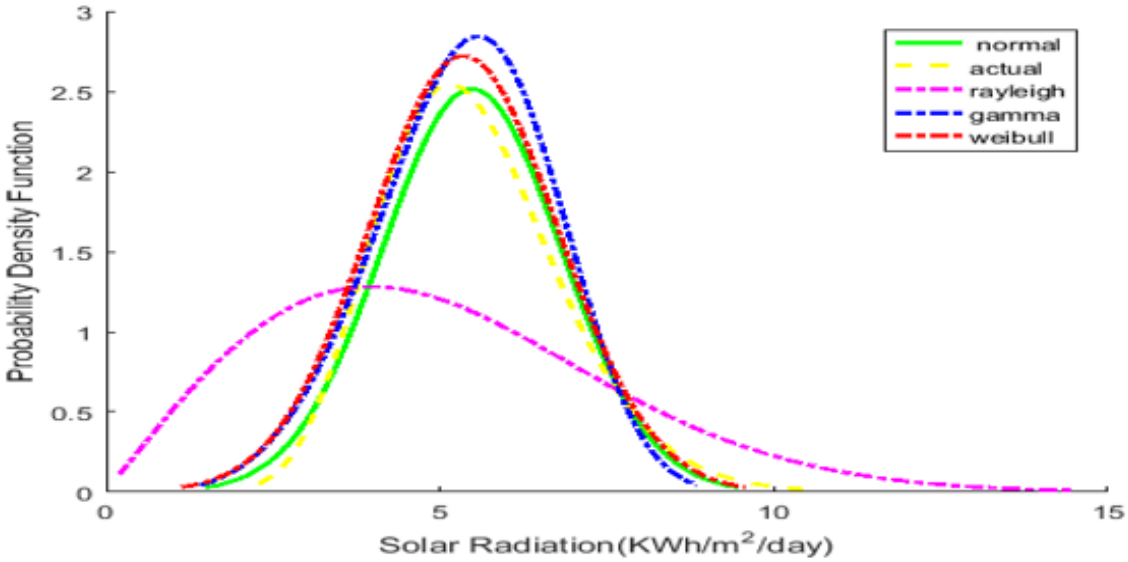

Figure 4.5: Fitting pdf to the actual data of Jalo

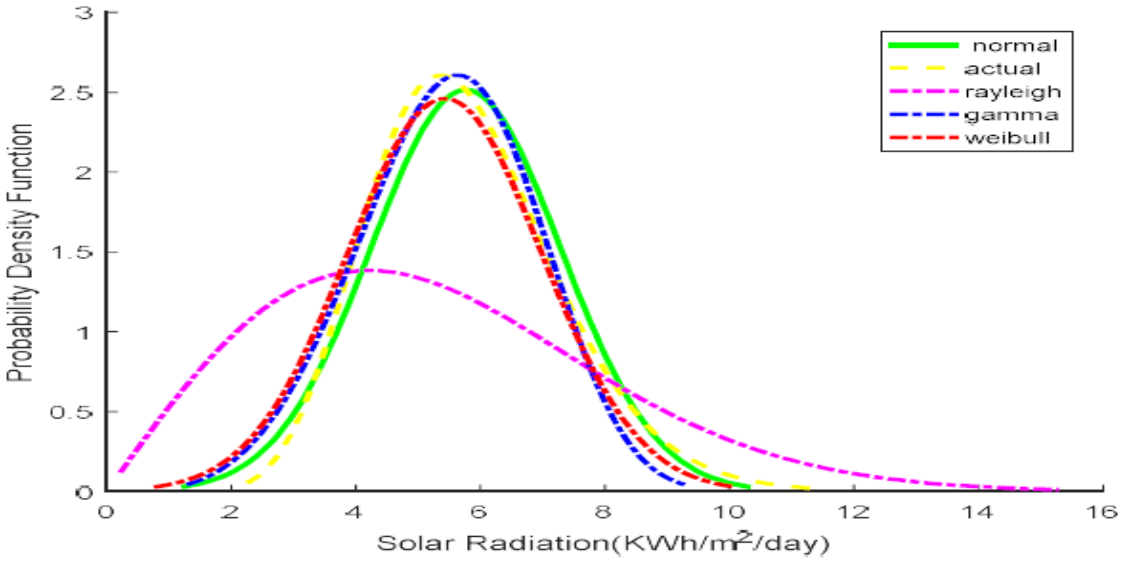

Figure 4.6: Fitting pdf to the actual data of Al-Kofra

CHAPTER 5

GRID-CONNECTED PHOTOVOLTAICS INTO THE LIBYAN POWER SYSTEM

Grid-connected PV systems have many technical advantages such as flexibility, simplicity to install in any area where solar irradiation is available, non-polluting, emitting no noise and requiring very little maintenance [42, 43]. Therefore, many countries are encouraging customers to install PV systems in order to generate some of their own power, to reduce electricity bills and to increase the contribution of renewable energy to limit carbon dioxide (CO_2) emissions. Ultimately, economics will play a significant role in determining the viability of adding large-scale PV in the Libyan power system. However, economic considerations should incorporate positive elements such as reducing carbon dioxide emissions on a local and global scale. Furthermore, the total generating capacity of Libya is 6,357 MW in 2013 [44]. This chapter presents a study of some of the potential impacts of the entry of grid-connected PV on the existing power system for the city of Hoon, Libya. Impacts on grid voltage and transmission losses including economic analysis are presented using two scenarios: Baseline scenario and PV MODEL scenario. Moreover, outputs of PV system can vary slowly or rapidly depending on climate conditions such as cloud cover, squall lines, etc. As a first step, grid-connected PV systems can be considered as negative load because of its uncontrollable features. With this background and limited literature, we discuss the large-scale entry of PV in the Libyan power system. Techno-economic feasibility of introducing large-scale grid-connected PV power plants (PV MODEL) into the Libyan power system and the impact on the reduction of carbon dioxide emissions as

Figure 5.1: Installed PV application projects in Libya [45, 14]

Table 5.1: Total installed PV capacity in Libya in 2006 [14, 46]

Applications	Number of systems	Total power, kWp
Communication	120	690
Cathodes protection	320	650
Rural Electrification	440	405
Water pumping	40	120
Roof Top	10	3
Total	1290	1868

it replaces to some extent conventional power plants are also discussed.

5.1 PV Applications in Libya

Photovoltaic conversion of insolation is a well-established technology. Libya is one of the developing countries in which PV was first put into operation in 1976 to supply electric power. Small PV projects have been in operation since 1976 in Libya as shown in Figure 5.1 . At first, solar systems were used to supply cathodic protection for the oil pipelines. Later, in 1980, a PV system was used in the communications sector to supply power to the microwave repeater station near Zalla.

By 2006, 120 stations powered by PV in the field of communications have been established in Libya. By the end of the year 2005, the total installed photovoltaic peak power was around 690 kWp [14]. In 2012, it rose to 950 kWp [14]. By 2012 the total capacity of PV water pumping system was 120 kWp [14, 46], as shown in Table 5.1

Figure 5.2: Installed PV application projects in Libya [14]

The use of PV systems for rural electrification in Libya was initiated in 2003 as shown in Figure 5.2. By 2006, the total number of remote systems installed by the General Electric Company of Libya GECOL reached 440 with a total capacity of 405 kWp. In 2012, rural electrification PV systems in Libya had an aggregated capacity of 725 kWp [46]. The Renewable Energy Authority of Libya is planning to implement a grid connected 14 MW photovoltaic power plant near the town Hun in Libya, a 40 MW project in Sabha, and a 15 MW power station in Ghat.

5.2 Electricity Demand

Due to high economic growth and greater investment in the oil and natural gas sectors, electricity generation almost doubled from 2003 to 2012 [16]. The peak load increased from 5,282 MW in 2009 to 5,981 MW in 2012 as shown in Figure 5.3. Figure 5.4 shows the load growth from 2013-2020, during which the total installed generation capacity increased to 8907 MW [13]. Despite growth in electricity generation and a high electrification rate, the country suffers from regular outages and the oil sector is also affected by power supply issues.

5.3 Electricity Consumption

In 2012, electricity consumption in Libya aggregated to 32.96 TWh, this corresponds to 4,850 kWh per capita as compared to only 2,650 kWh in the year 2000 on an annual basis as shown in Figure 5.5. Most of the electric power network is concentrated in the coast, where most of the inhabitants live.

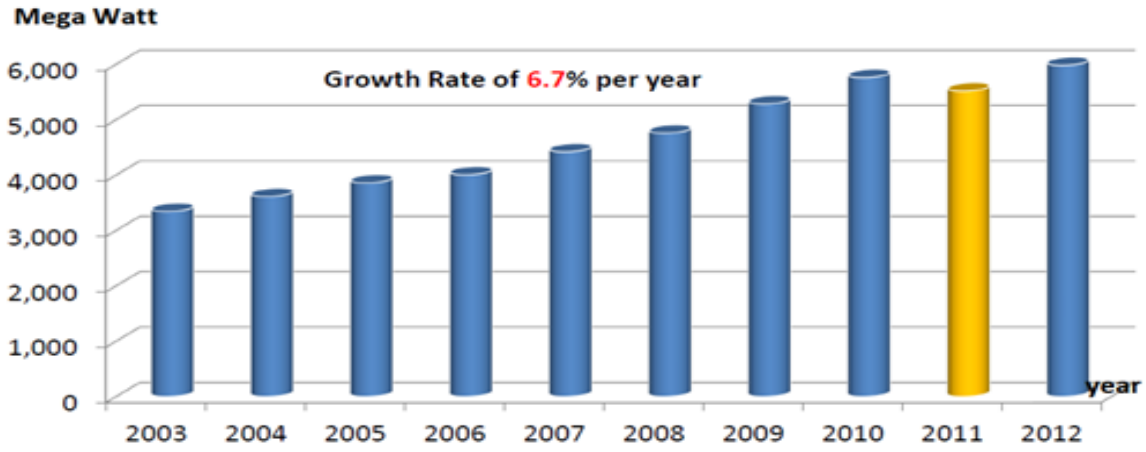

Figure 5.3: The peak load growth within 2003 —2012 [13]

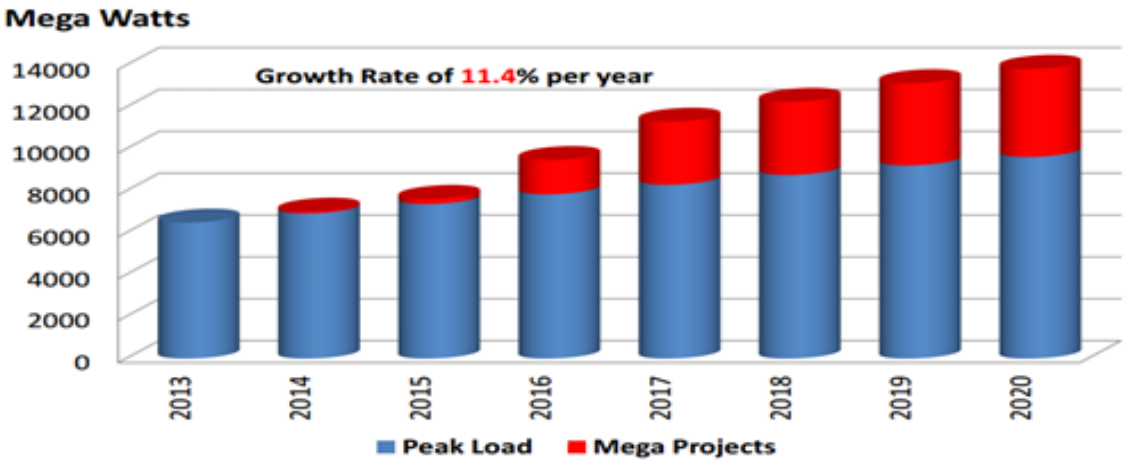

Figure 5.4: Load growth within 2013 —2020 [13]

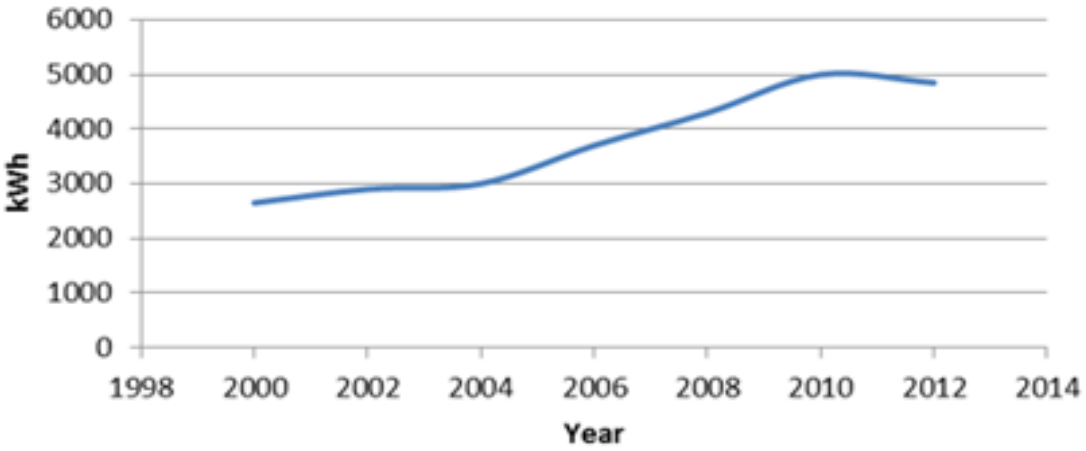

Figure 5.5: Anuual electrical power percapita consumption of Libya [13]

5.4 Environmental Effects

The major emitters of CO2 in Libya, as shown in Figure 5.6, are fossil fuel burning power plants at 40%, in the transport sector 22%, and in manufacturing sector 10% and all others combined 28%. Carbon emission from petroleum products stand at 58% and from natural gas 42% [16].

Increasing dependence on natural gas will lead to less carbon emissions. Libya's contribution regarding CO2 emissions has increased due to growth in energy sector over the years. Continued combustion of fossil fuels for power generation leads to very

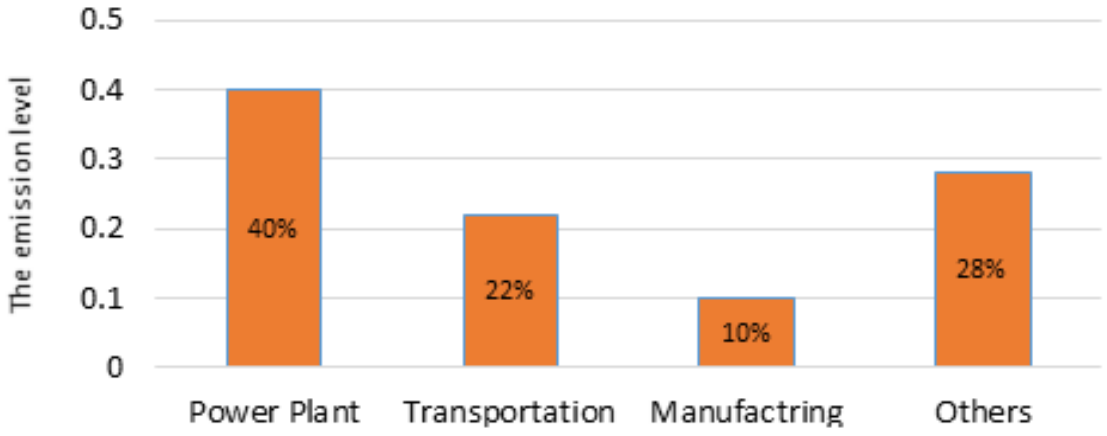

Figure 5.6: CO2 emission by sectors in Libya [16, 13]

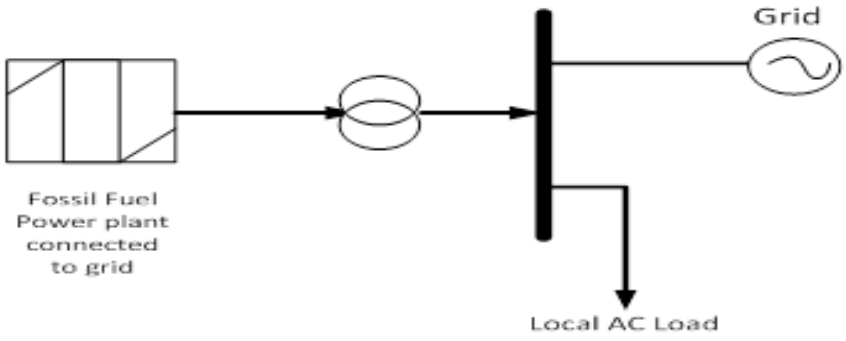

Figure 5.7: The conventional power plant

high environmental pollution and global warming problems since currently more than 70% of the power is generated using fossil fuels. Fast depletion of traditional fuels with limited resources is another matter of concern about growing energy demand. Development of renewable energy is promoted as a green solution in some developing countries such as Libya with the aim of mitigating emission issues and satisfying upcoming energy demand. Recently renewables accounted for 15–20% of the world's total energy needs [47]. Libya is taking steps towards major actions in the country such as approving the Kyoto protocol to the UN convention on climate change and having a target of achieving 10% renewable energy power generation by 2020. One possible approach in Libya is to employ smart integrated renewable energy systems (SIRES) [48].

5.5 Baseline Model

Developed countries have supplied electric power generated in large centralized plants transforming and transmitting at high voltages to regional consumers, step it down to distribute it locally and deliver it to customers as seen in Figure 5.7

A combination of electricity generation by means of PV, used to replace some amount of electricity where conventional energy sources are expensive or rarely available, is expected to improve the prospects for harnessing the free and clean solar

energy in an economical way. The integration of these units together can reduce the overall heat rate of the entire generation system significantly. This would reduce the cost of the generated electricity compared with what can be achieved with stand-alone conventional units. In addition, lower rates of emissions per unit of electricity produced would be beneficial to the environment. Direct generation of power from fossil fuel fired power plant has several negative effects on the environment since CO_2 emissions contribute to greenhouse effect.

5.6 PV Model

Integration of PV into the Libyan power system has the potential to provide a reduction of the overall operating cost of the system. This is because insolation is free, while fuel oil and natural gas are not. By using less oil and natural gas, emission of CO_2 decreases. This system consists of photovoltaic (PV) power plants to generate clean electricity by using solar energy, incorporated with fossil fuel power plants and feed-in the generated electricity into the grid to supply the growing peak demand of customers as shown in Figure 5.8

The random variable solar irradiance as insolation can be modeled using the Beta probability density function [49]. The probability density function for solar irradiance can be expressed as follows:

$$f_b(s) = \begin{cases} \frac{\Gamma(\alpha+\beta)}{\Gamma(\alpha)\Gamma(\beta)} s^{\alpha-1} \\ *(1-s)^{(\beta-1)}, & for 0 \leq s \leq 1, \alpha, \beta \geq 0 \\ 0, & otherwise \end{cases} \tag{5.1}$$

where f_b (s) is the Beta distribution function of s, and s is the random variable of solar irradiance in kW/m2, β and α are parameters of f_b (s), which can be found using the mean μ and standard deviation σ of "s" as follows:

$$\beta = (1-\mu)\left(\frac{\mu(1+\mu)}{\sigma^2} - 1\right) \tag{5.2}$$

$$\alpha = \frac{\mu \times \beta}{1-\mu} \tag{5.3}$$

5.7 Technical Analysis

Simulation results obtained using the power world simulator employing the Newton Raphson approach are summarized in this section. The buses used in power world simulator were classified as generation bus, load bus and slack bus. The system under study shown in Figure 5.9 is a typical distribution system and it displays the model of a sample eleven bus network built using the power world simulator. The information consists of bus voltages for every node assumed to be within the acceptable range between 0.95 and 1.05 per unit. Bus 1 is considered as the slack bus, buses 2, 3, 4, 5, 6, 8, 9, 10, 11, and 13 are load buses. The system has a total active and reactive power load of 173.54 MW and 84.08 MVAR respectively. The generator at bus one

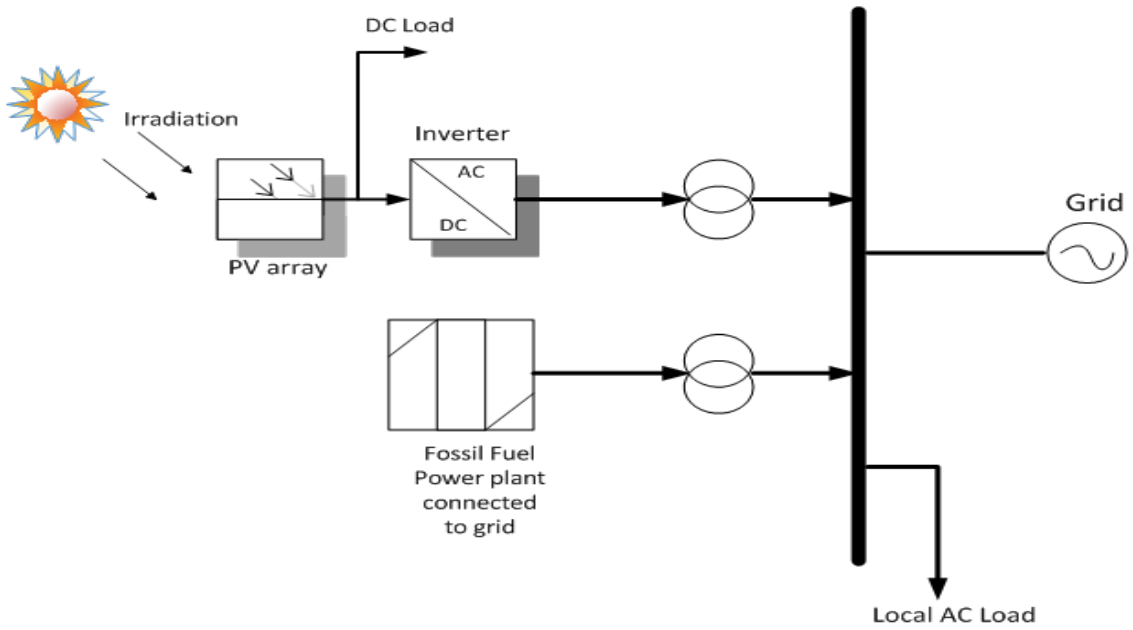

Figure 5.8: Hybrid Photovoltaic and fossil fuel system

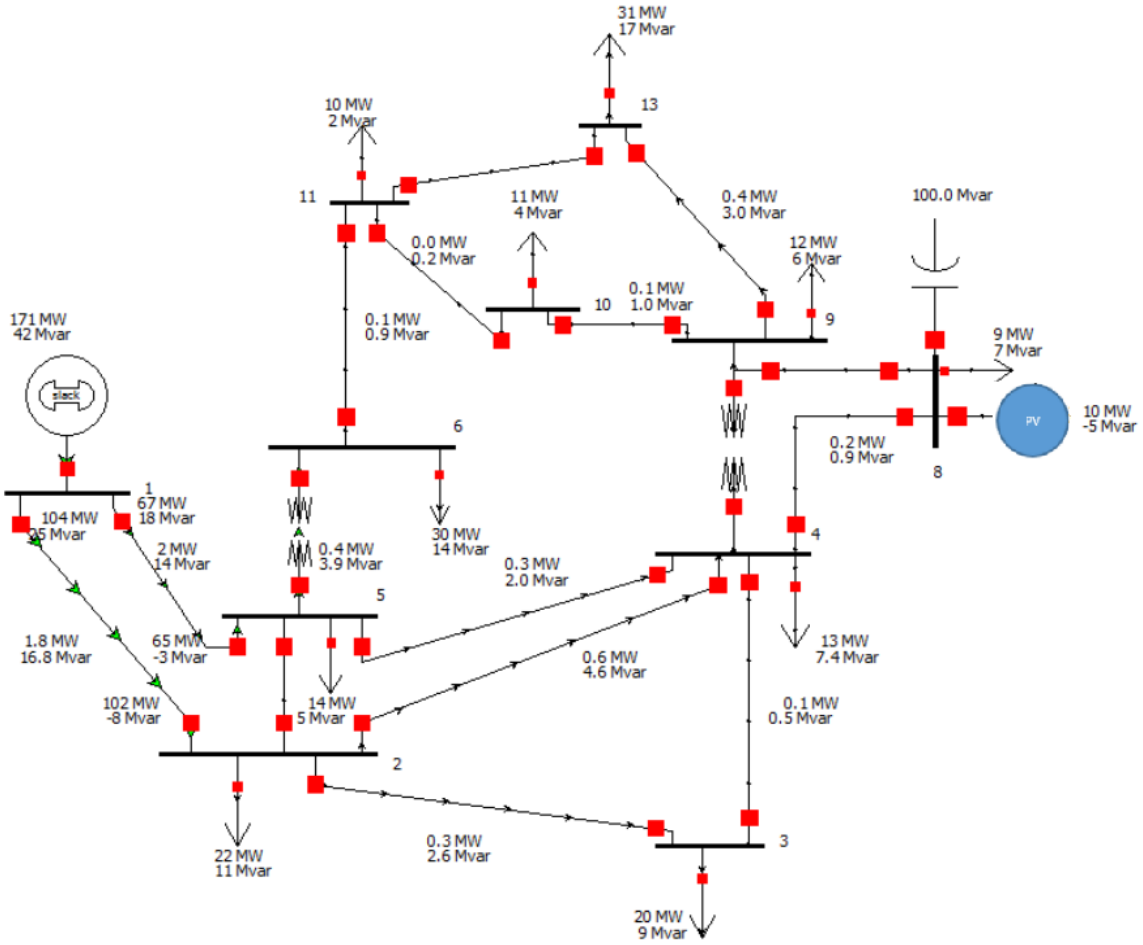

Figure 5.9: Proposed PV Model consisting of ten loads and existing power generation

generates 182.51 MW and the transmission lines connected between buses are shown in the single-line diagram. The generator‘s real and reactive power are assumed to vary within certain limits to meet a particular load demand with minimum fuel cost based on Optimum Power Flow (OPF). Optimal power flow plays an important role in power system operations and planning. Under normal operating condition, OPF is used to determine the load flow solution, which satisfies the system operating limits with minimum generation costs.

Distributed photovoltaic generation dispersed throughout the network can supply a part of the power demanded by the load. Varying percentages of photovoltaic penetration level are considered in this study using power world simulator to simulate

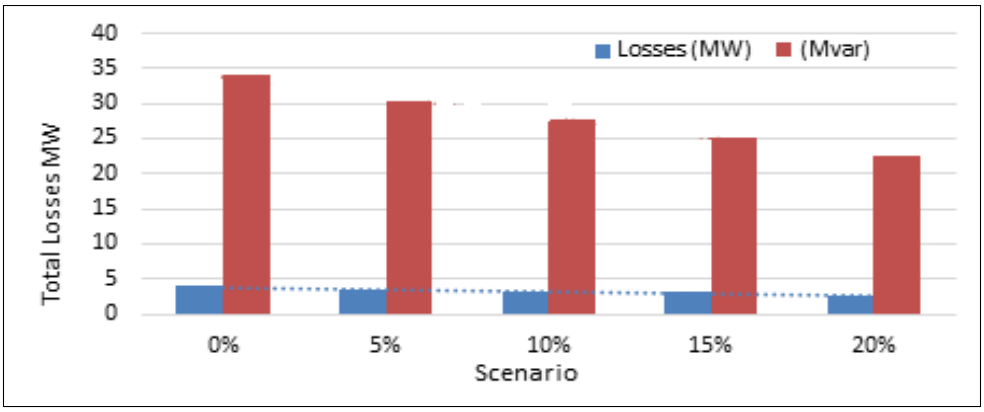

Figure 5.10: Total losses of the system for different scenarios

the system. A power flow analysis is run for each of the scenarios. Evaluation of the performance of the proposed system is done by comparing every scenario with the base scenario (with no PV) in terms of total losses and total generation and the results of the simulation are illustrated in Figures 5.10 and 5.11.

To evaluate the impact of PV penetration, the following scenarios are considered:

Scenario 1: A PV of 5% (10 MW).

Scenario 2: A PV of 10% (18 MW).

Scenario 3: A PV of 15% (27 MW).

Scenario 4: A PV of 20% (36 MW).

In each case the PV system is assumed to be at bus 7 as shown in Figure 5.9. Compared to the base scenario, the PV Model resulted in a reduction of total existing generation from 178.51 MW to 167.91 MW, 159.71 MW, 150.61 MW, and 141.11 MW for the scenario of 1, 2, 3, and 4, respectively, as shown in Figure 5.11. In addition, Figure 5.10 also shows the total losses obtained from the simulation of the system. It decreased from 4.0 MW to 3.4 MW, 3.2 MW, 3.1 MW and 2.1 MW for the scenario of 1, 2, 3 and 4 respectively.

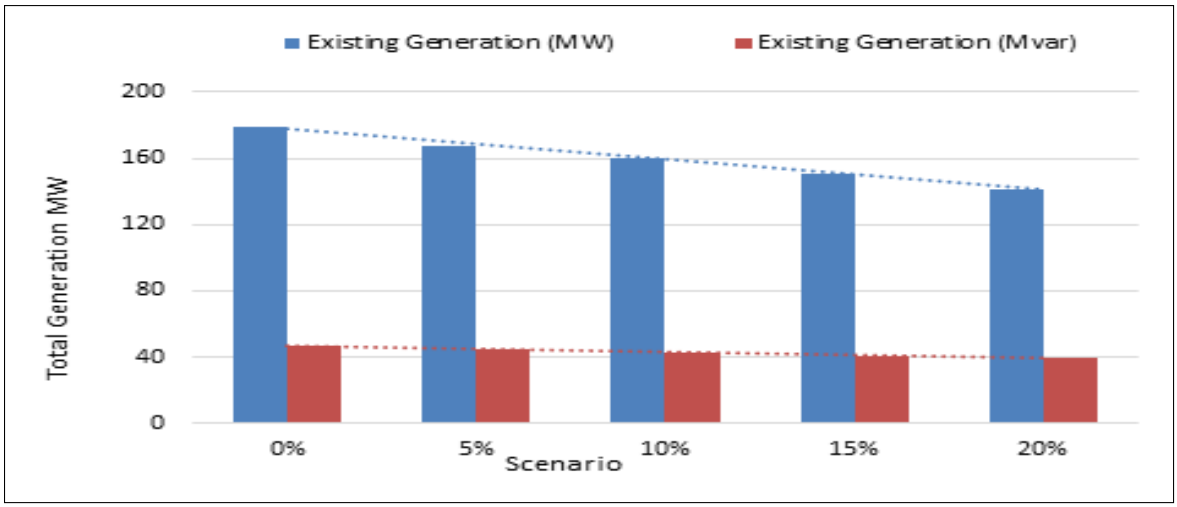

Figure 5.11: Total existing generation for different scenarios

CHAPTER 6

IMPACT OF PV INTEGRATION ON THE LIBYAN POWER SYSTEM

Global interest in curbing greenhouse gas emissions, especially carbon dioxide, is on the rise as exhibited by the unprecedented accord arrived at in Paris in December 2015 by 196 delegates from all around the world, known as COP 21. The goal was to take measures to limit average warming to no more than 2 degrees Celsius above pre-industrial temperatures, with a desire to strive for 1.5 degrees Celsius if possible [32]. Moreover, cost of photovoltaic (PV) modules has been declining significantly at an average rate of 20% with each doubling of sales. With this background, this chapter considers the impact of PV penetration into the Libyan power grid. In particular, impacts on grid voltage and transmission losses are studied. Baseline and PV model scenarios are considered for their impact on carbon dioxide emissions resulting from the operation of conventional power plants in the Libyan power system. The results of this study will aid the acceleration of developing PV power plants over conventional power generation technologies in the Libyan power system from both technical and economics perspectives.

The Renewable Energy Authority of Libya (REAOL) and the Center for Solar Energy Studies (CSES) started looking for engineering experts to help the company assess the country's solar energy resources and design the first commercial photovoltaic power plant in the city of Al-Kofra. Libyan electricity utility established the Renewable energy authority of Libya (REAOL) to promote the development of renewable energy resources. The electricity generated will be injected into the Libyan

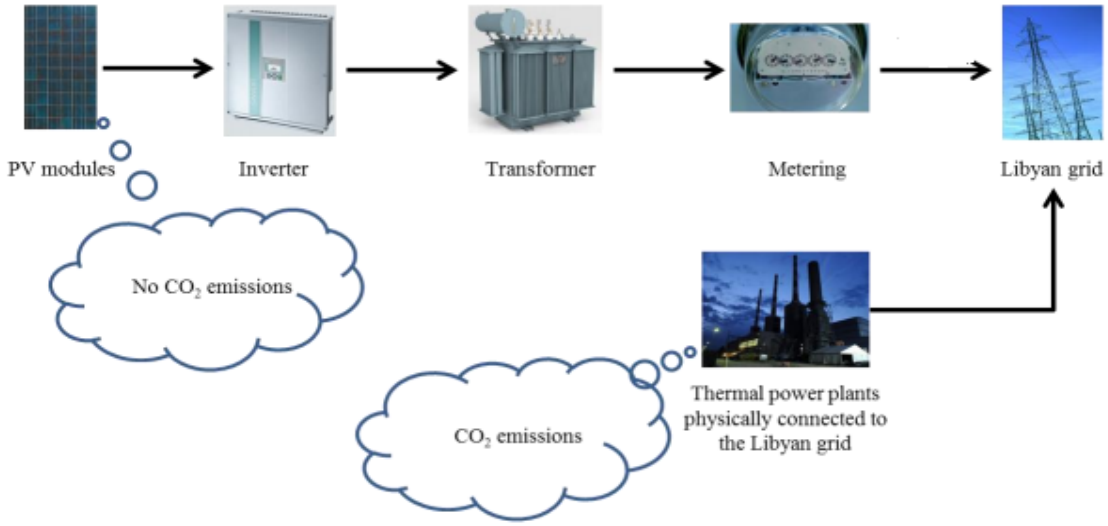

Figure 6.1: Electricity generated supplied to the national grid [50]

national electricity grid, as illustrated in Figure 6.1. The photovoltaic power plant will employ state-of-the-art PV modules, inverters, transformers, protection systems and supporting components for electricity generation and for proper integration with the Libyan grid.

6.1 Approach

Growing population is causing significant growth in power demand in Libya, which needs far more investment in the infrastructure such as power lines and additional power stations. Furthermore, industrial growth is demanding nonstop 24/7 operation of power plants and increasing fuel consumption. This gives a strong impetus to study the feasibility and importance of renewable energy in Libya. This chapter investigates the impacts of photovoltaics penetration into the Libyan power system and the possibility of its utilization in Libya.

6.2 Effects of PV on Traditional Power System

The steadily decreasing cost of PV modules creates an economic incentive for grid-connected PV systems. Also, the operation and maintenance cost of PV is rather low. Energy costs from PV plants will approach that from conventional plants in the near future. The market for renewable energy will increase faster than for conventional fossil fuel power plants.

6.3 Methodology

The existing power plant considered in this chapter mainly refers to the city of Al-Kofra, located in the largest district of Libya. Its capital is Al-Jwawf, one of the oasis in Al-Kofra basin with coordinates (23.3112° N, 21.8569° E) [51]. Al-Kofra is located about 857 miles away from the capital of Libya, Tripoli, with a population of 157,747 inhabitants and a total area of 433,611 mi^2. The generation capacity of the existing power plant is 150 MW. The grid connection will be less than 100 meters away from the proposed site as illustrated in Figure 6.2. The substation (66 kV/11kV) has two transformers, 20 MVA each.

The study was conducted using two scenarios. The first scenario is the baseline scenario based on existing power generating system, and the second scenario, PV MODEL, was established to investigate the feasibility of introducing large-scale PV. Scenarios were constructed and studied using PowerWorld Simulator, a Windows-based software that has been developed by the PowerWorld Corporation located in Champaign, Illinois, USA. The software is an interactive power system simulation package designed to simulate high voltage power system operation on a time frame ranging from several minutes to several days and contains a highly effective power flow analysis package capable of efficiently solving systems of up to 250,000 buses. Therefore, among other power network data analysis hardware and algorithms (e.g.

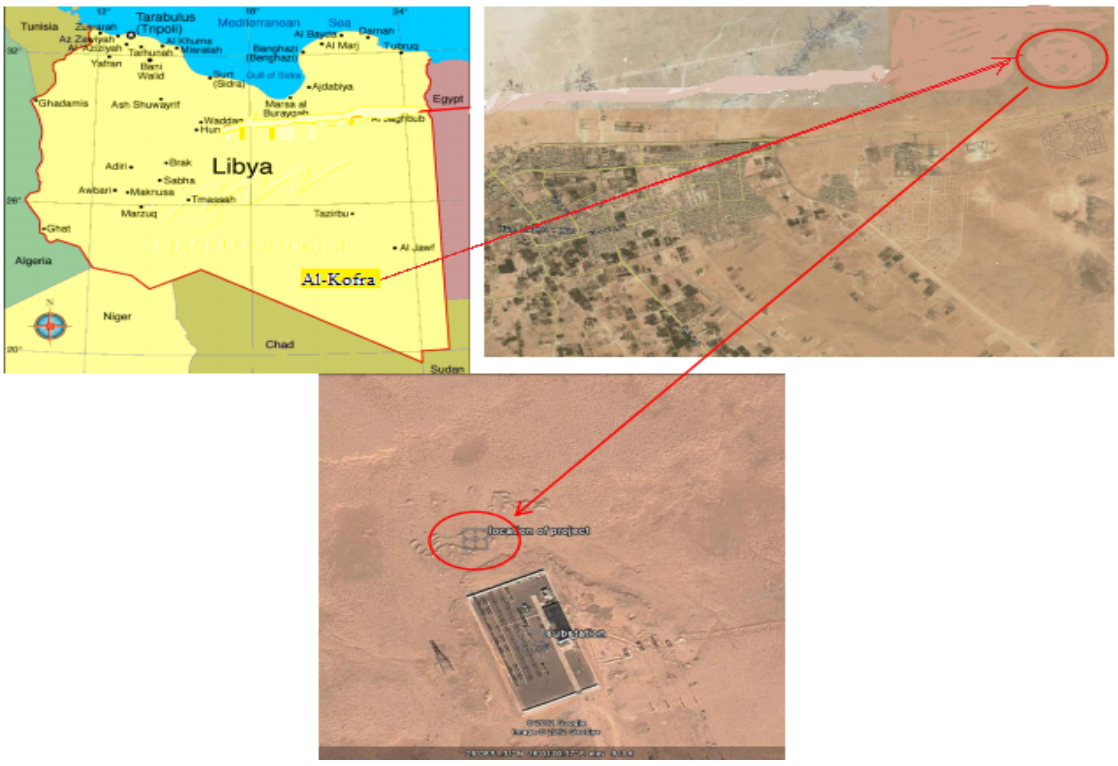

Figure 6.2: The location for the proposed project activity of Al-Kofra [51]

Matlab, LabView), PowerWorld offers substantial advantages, including an easier to develop different network scenarios and more appropriate to analyze power networks consisting of smart grid technologies and active components [52]. Two scenarios were constructed based on the current power system and the PV MODEL that uses PV power plant in medium to large-scale capacity throughout the districts of AL-Kofra. A bus is a point or node where transmission lines, loads, and generators are interconnected. Typically, a bus is associated with four elements. They are voltage $|V|$, phase angle of voltage (δ), active power (P), and reactive power (Q). Two parameters of each of the buses are already defined, while the rest should be calculated. In power flow study, buses ae categorized into three types: slack bus, generator bus (PV bus), and load bus (PQ bus). The slack bus contains information of $|V|$ and δ, while PV bus includes defined P and $|V|$, and PQ bus covers P and Q [53, 54]. In the present study, total Bus-bars (11 Bus-bars) and transmission lines (13 lines) were simulated

and solved using Newton-Raphson method. Provided in the software and typically expressed as described in Eq. 6.1 to 6.4, where S_i, P_i, and Q_i represent the apparent, real, and reactive powers. All Transmission lines were assumed to use common conductor types, aluminum conductor, steel reinforced (ACSR) and the line data refers to the system at Al-kofra.

$$S_i = V_i I_i^* = V_i \left(\sum_{k=1}^{n} Y_{ik} V_k \right)^* = V_i \sum_{k=1}^{n} Y_{ik}^* V k^* \tag{6.1}$$

$$\begin{aligned} S_i = P_i + jQ_i = V_i \sum_{k=1}^{n} Y_{ik}^* V_k^* &= \sum_{k=1}^{n} |V_i||V_k| e^{j\delta_{ik}} (G_{ik} - JB_{ik}) \\ &= \sum_{k=1}^{n} |V_i||V_k| (\cos\delta_{ik} + j\sin\delta_{ik})(G_{ik} - jB_{ik}) \end{aligned} \tag{6.2}$$

$$P_i = \sum_{k=1}^{n} |V_i||V_k| (G_{ik}\cos\delta_{ik} + B_{ik}\sin\delta_{ik}) = P_{Gi} - P_{Di} \tag{6.3}$$

$$P_i = \sum_{k=1}^{n} |V_i||V_k| (G_{ik}\sin\delta_{ik} + B_{ik}\cos\delta_{ik}) = Q_{Gi} - Q_{Di} \tag{6.4}$$

6.4 The Baseline Scenario

The baseline scenario is the current power grid system in the city of Al-Kofra, Libya that consists of 10 substations with a total load of 144 MW (gross) and a combined cycle power plant (CCPP) that uses natural gas as the primary fuel. The CCPP operates two gas turbines and one steam turbine run on either natural gas or diesel fuel (dual fuel gas turbine) producing 130 MW in total. The gas turbines have a combined nameplate capacity of 84 MW (gross) and characteristics similar to GE Frame 6B gas turbine unit [55], while the steam turbine has a nameplate capacity of 50 MW [56]. Detailed specifications of the gas turbine and steam turbine are shown

Table 6.1: The specification of current power generation units [56, 55]

Power Production Unit	Description
Gas turbine, GT	
Manufacturer	General Electric, GE
Fuel type	Natural gas/ high speed diesel
Number of gas turbine	2
Nameplate capacity, MW	42 (each)
Type of combustor	DLN
Number of compressor stage	17
Exhaust temperature, $^{\circ}C$	549
Maintenance interval, hours	32,000
Heat recovery steam generator, HRSG	
Manufacturer	Thermax Babcock Wilcox
Type of design	Vertical flow structure
Number of HRSG	2
Unfired, normal and maximum rating, tons per hour	66, 78, and 86 (tph)
Steam temperature, $^{\circ}C$	535
Steam turbine, ST	
Manufacturer	Shin Nippon Machinery
Nameplate capacity, MW	50
Maximum inlet steam pressure, kg/cm^2	130

in Table 6.1. The CCPP has an estimated plant heat rate of 8,500 Btu/kWh. This CCPP power plant designated as slack bus under the baseline scenario. The power grid system uses base values of 138 kV, 100 MVA and 50 Hz of frequency.

The substations within the district have different load profiles, divided into two categories: 11 MW and 22 MW of load, where the higher load demands (22 MW) are located in southern part of the system. Parameters of the transmission lines are listed in Table 6.2. It consists of 13 lines with resistance and reactance (R and X) values as listed. Two transformers used in this system connect Bus-bar 5 to 6 and the other Bus-bar 4 to 7. Additional technical and operational details are listed in Table 6.3.

Table 6.2: The transmission profile of the system under baseline scenario

The transmission line	Series resistance, R	Series reactance, X
1 (Busbar 1 to 2)	0.016	0.147
2 (Busbar 1 to 5)	0.040	0.300
3 (Busbar 2 to 3)	0.040	0.300
4 (Busbar 2 to 4)	0.040	0.300
5 (Busbar 2 to 5)	0.040	0.300
6 (Busbar 3 to 4)	0.040	0.300
7 (Busbar 5 to 4)	0.040	0.300
8 (Busbar 6 to 9)	0.040	0.300
9 (Busbar 6 to 10)	0.040	0.300
10 (Busbar 7 to 8)	0.040	0.300
11 (Busbar 7 to 11)	0.040	0.300
12 (Busbar 8 to 9)	0.040	0.300
13 (Busbar 11 to 10)	0.040	0.300

Table 6.3: The transformer profile used in the system

Transformer	Technical description	Operational mode
Busbar 5 to 6	Series resistance, R = 0.016; Series reactance, X = 0.147; Size = 4.2 MVA, Min. tap ratio = 0.9, Max. tap ratio = 1.1	Automatic control enabled: Voltage regulation (Min.: 0.99; Max.: 1.01)
Busbar 4 to 7	Series resistance, R = 0.020; Series reactance, X = 0.040; Size = 4.6 MVA; Min. tap ratio = 0.9, Max. tap ratio = 1.1	Automatic control enabled: Voltage regulation (Min.: 0.99; Max.:1.01)

6.5 PV Model Scenario

PV MODEL involves the use of the high solar intensity in the region of Al-Kofra, with a higher intensity of ($7.51 kWh/m^2/day$), more than other regions in Libya ($4.4 - 6.40 kWh/m^2/day$) [57]. In addition to system performance, emission reduction resulting from the use of PV are evaluated. PV has zero CO_2 emission and it reduces the consumption of natural gas by CCPP power plant [58]. The detailed PV specifications are shown in Table 6.4 with maximum efficiency of 17% and power output range of 260 to 280 watt for each panel. Although the maximum efficiency of PV can reach 33% [59], however, a typical efficiency achieved in commercial practices

Table 6.4: Detailed specifications of solar PV used in this work [60]

Manufacturer	Trina Solar
Power output range, watt	260 to 280
Maximum Efficiency, %	17
Positive power tolerance, %	0 to 5
Cell orientation	60 cells (6 x 10)
Module dimensions	1664 x 998 x 7.6 mm
Weight, kg (lb)	23.5 (51.8)
Nominal operating cell temperature, $^{\circ}C$	44
Maximum rating of temp. $^{\circ}C$	-40 to 85

is around 15-19% [60].

6.6 Results and Discussion

6.6.1 Model Convergence

Both models (PV MODEL 1 and PV MODEL 2) including the existing power system were simulated using Newton-Raphson method. The convergence of the models was obtained after three iterations as shown in Figure 6.3. As typically known, the more complex of a power system, more iteration might be required to run the simulation with accurate results.

6.6.2 Baseline Scenario

Single-line diagram of the current power system in the district of Al-Kofra is shown in Figure 6.4. It can be observed that the presence of existing CCPP dominants the entire power grid across the areas of Al-Kofra. The simulation resulted in the power generating capacity of the current CCPP of 139 MW, considered as slack bus, which was close to the actual capacity of existing CCPP (150 MW). A power flow of 84 MW (19 MVar) delivered from the CCPP (Bus-bar 1) to substation 9 (Bus-bar 2), and power flow of 54 MW (16 MVar) supplies the substation 1 (Bus-bar 5). Moreover, as aforementioned, substations located in Southern part consumed more

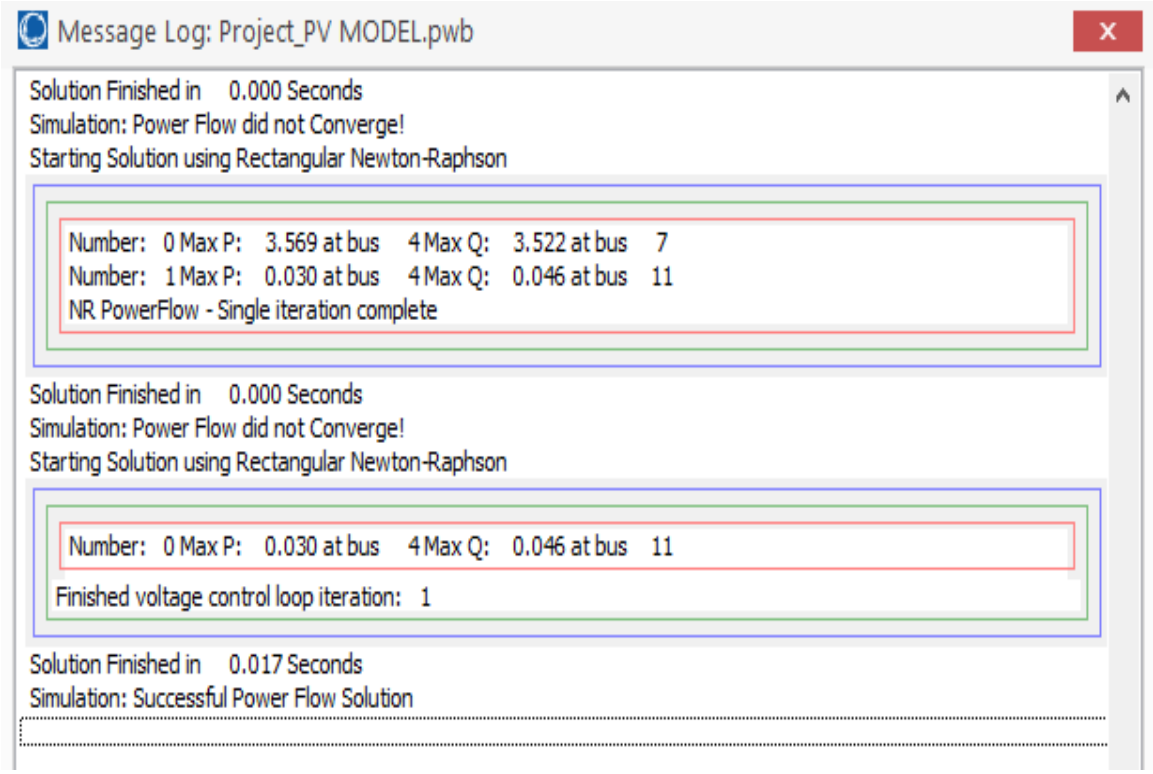

Figure 6.3: Snapshot of model convergence of PWS simulation

power than the northern part of the district. Since the northern part of the district also received power from the existing power plant (CCPP), it was not necessary to clearly investigate which parts of the region are critical zones, which could be indicated either by the highest voltage drop or by the biggest transmission losses in the power grid. The critical zone will be the most suitable area to apply the PV MODEL since the PV MODEL will either stabilize the power grid (e.g. voltage rating) or minimize the transmission losses within the power grid. To further analyze the power system, it was necessary to observe the power flow within the system as shown in Figure 6.4. Power flows including transmission losses and voltage rating within the system (e.g. Bus-bar) are listed in Table 6.5. As can be observed, it was most effective to install PV in the region of either Bus-bar 3 or Bus-bar 5, as compared to other regions since those areas had the lowest voltage rating (0.95 and 0.94 p.u respectively). To confirm these results, an additional load can be simulated to the targeted Bus-bar to test the

profile of the transmission load. The simulation resulted in an overload that occurred in the transmission line between Bus-bar 1 to 2 when the load at Bus-bar 3 increases to 40 MW, causing the voltage drop into the value of 0.91 p.u as shown in Figure 6.5.

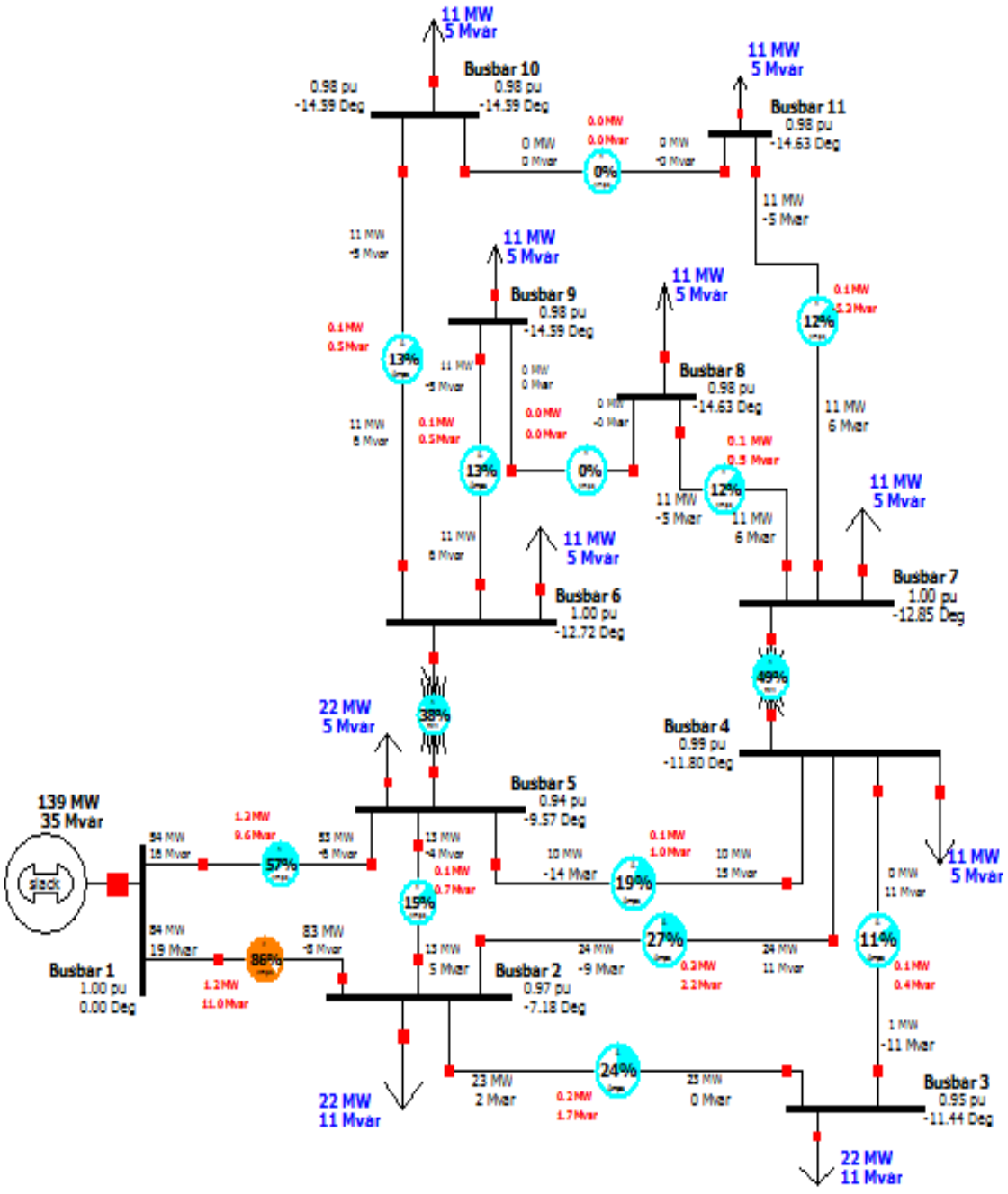

Figure 6.4: The baseline scenario of the current power system

A similar condition was found if the increasing load was applied at Bus-bar 5,

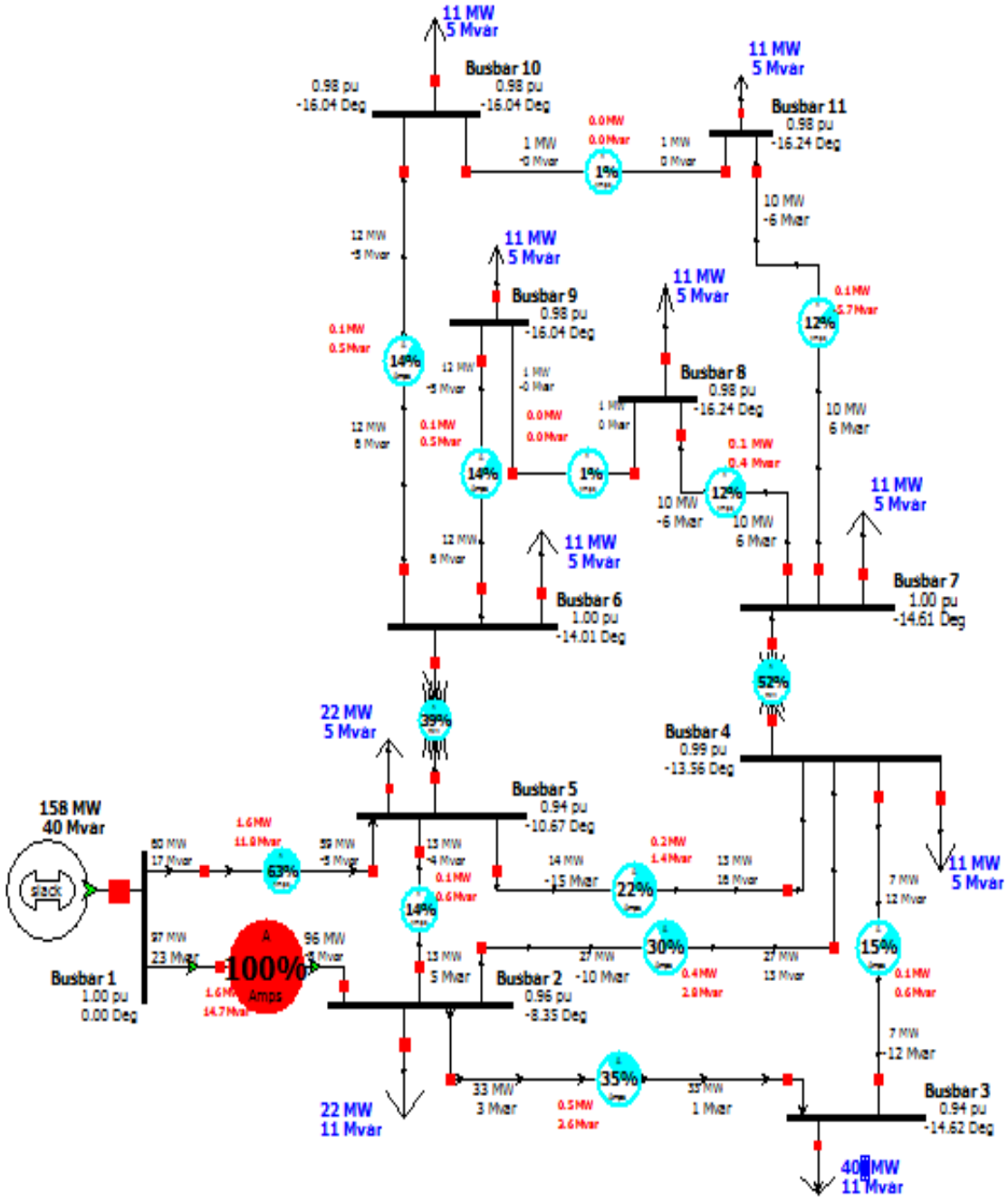

Figure 6.5: Overload condition of the transmission line 1 (Busbar 1 to 2)

from 22 MW to 48 MW, that caused an overload (100%) in transmission line 1 (Bus-bar 1 to 2). Since Bus-bar 3 is more sensitive to the increasing load of the system (40 MW causing an overload condition to the transmission line 1) than Bus-bar 5 (48 MW causing overload condition to the transmission line 1), the new PV power

Table 6.5: Overload condition of the transmission line 1 (Busbar 1 to 2)

Transmission line	Power Flow	Transmission losses	Busbar	
			No	Voltage p.u.
1	Bus 1 to 2	1.2 MW; 11.0 MVar	1	1.00
2	Bus 1 to 5	1.2 MW; 9.6 MVar	2	0.97
3	Bus 2 to 3	0.2 MW; 1.7 MVar	3	0.95
4	Bus 2 to 4	0.3 MW; 2.2 MVar	4	0.99
5	Bus 2 to 5	0.1 MW; 0.7 MVar	5	0.94
6	Bus 3 to 4	0.1 MW; 0.4 MVar	6	1.00
7	Bus 5 to 4	0.1 MW; 1.0 MVar	7	1.00
8	Bus 6 to 9	0.1 MW; 0.5 MVar	8	0.98
9	Bus 6 to 10	0.1 MW; 0.5 MVar	9	0.98
10	Bus 7 to 8	0.1 MW; 0.5 MVar	10	0.98
11	Bus 7 to 11	0.1 MW; -5.3 MVar	11	0.98
12	Bus 8 to 9	0.0 MW; 0.0 MVar	-	-
13	Bus 11 to 10	0.0 MW; 0.0 MVar	-	-

plant (PV MODEL) was expected to be constructed in the region of Bus-bar 3 (top priority) and Bus-bar 5 (second priority). The additional explanation of the load variation was also addressed by [52] that the increase of load due to increased power demand directly increases the current and as a result, the voltage drop caused by the line and transformer impedance will be dominant. A detailed profile of the entire power grid system, expressed as the Model Explorer, is shown in Table 6.6. It can be inferred from the Model explorer that the largest voltage drop of the system occurs at Bus-bar 3 and 5, to values of 131.5 and 130.3 kV, respectively. The results were in agreement with the previous observation that new PV solar power was recommended to be installed in the region of Bus-bar 3 in order to reduce the voltage drop and minimize transmission losses. In addition, from 138.66 MW of total power generated from the power plant, about 2.6 MW of total losses was observed, representing about 1.8% of total losses.

Table 6.6: Model explorer of the current power system

Name	Nom kV	PU Volt	Volt (kV)	Angle (Deg)	Load MW	Load MVar	Gen MW	Gen MVar
Bus 1	138	1	138	0			138.66	35.01
Bus 2	138	0.96	133.23	-7.18	22.26	10.78		
Bus 3	138	0.95	131.55	-11.44	22.26	10.78		
Bus 4	138	0.98	136.21	-11.8	11.13	5.39		
Bus 5	138	0.94	130.37	-9.57	22.13	5.39		
Bus 6	138	1.00	138.14	-12.72	11.00	5.00		
Bus 7	138	1.00	138.00	-12.85	11.00	5.00		
Bus 8	138	0.97	135.07	-14.63	11.13	5.39		
Bus 9	138	0.97	135.11	-14.59	11.13	5.39		
Bus 10	138	0.97	135.11	-14.59	11.13	5.39		
Bus 11	138	0.97	135.07	-14.63	11.13	5.39		

6.7 PV Model Scenario

By introducing solar power to the current power grid, the PV MODEL was expected to reduce the generating capacity of the existing CCPP, yet improving the voltage profile of the system. In addition, the new PV solar power in the system could greatly reduce the consumption of natural gas fuel by the existing Power plant.

A 10 MW PV solar power plant was added and connected to the system as shown in Figure 6.6. The first model (PV MODEL 1) locates all the PV addition at Bus-bar 3 (total 10 MW), while the second model (PV MODEL 2) will divide the Solar PV in two locations, 5 MW at Bus-bar 3 and 5 MW at Bus-bar 5 (total 10 MW).

PV MODEL 1 resulted in an increase of Bus-bar 3 voltage (from 0.95 to 1.00 p.u) as shown in Table 6.7 and a decrease of the transmission load on the capacity of transmission line 1 (from 86% to 78%) as shown in Figure 6.6. It also reduces the transmission load of the transmission line 2 (from 57% to 52%). On the other hand PV MODEL 2 increases the voltage of Bus-bar 3 (from 0.95 to 1.00 p.u), Bus-bar 5 (from 0.94 to 1.00 p.u) as listed in Table 6.7 and decreases the transmission load of the transmission line 1 (from 86% to 77%). It also reduces the transmission load of the transmission line 2 (from 57% to 50%). Thus, PV MODEL 2 seems to offer more

advantages to the current power system in terms of voltage profile and transmission load reduction as detailed in Figure 6.7.

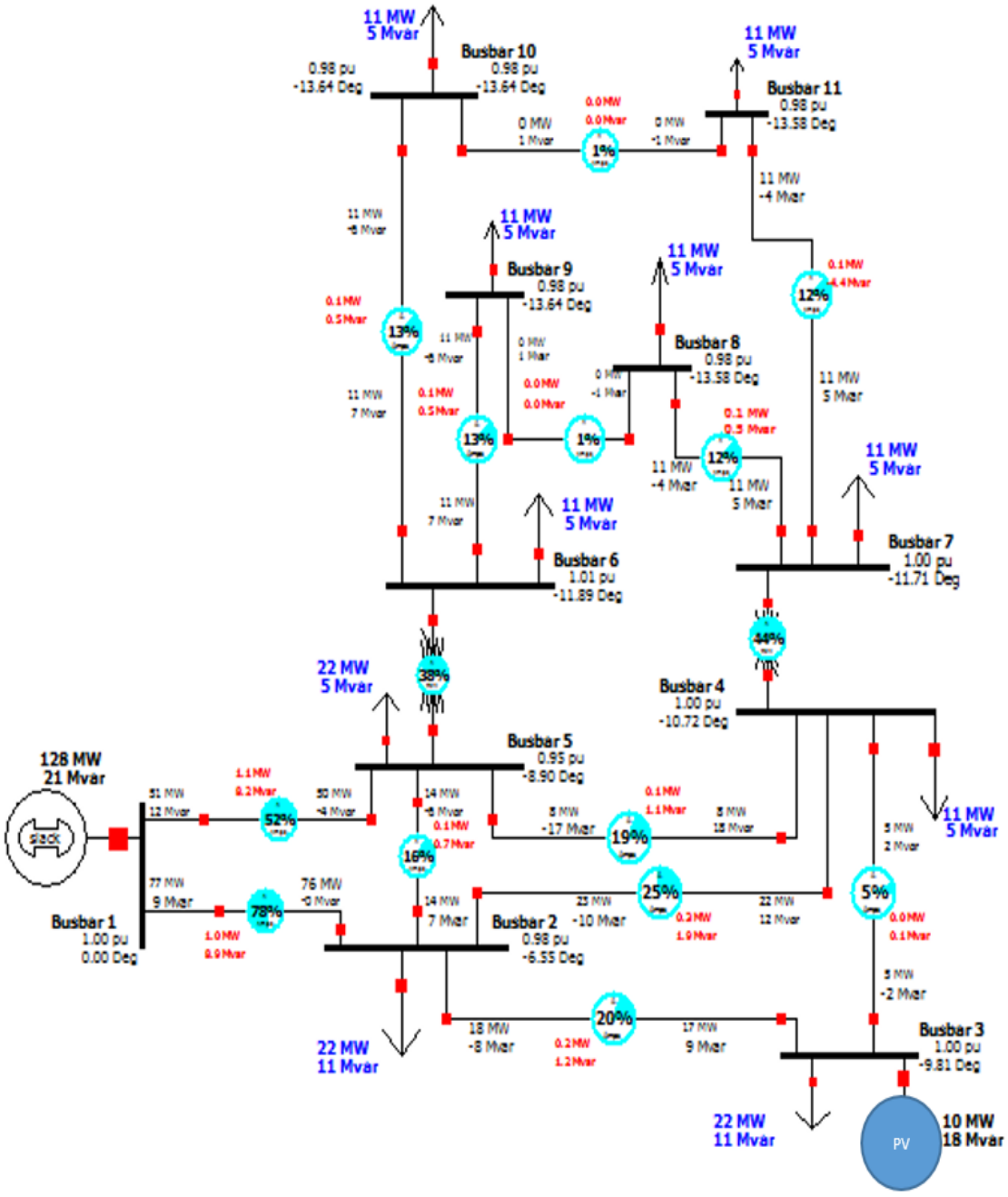

Figure 6.6: Simulation result of PV MODEL 1

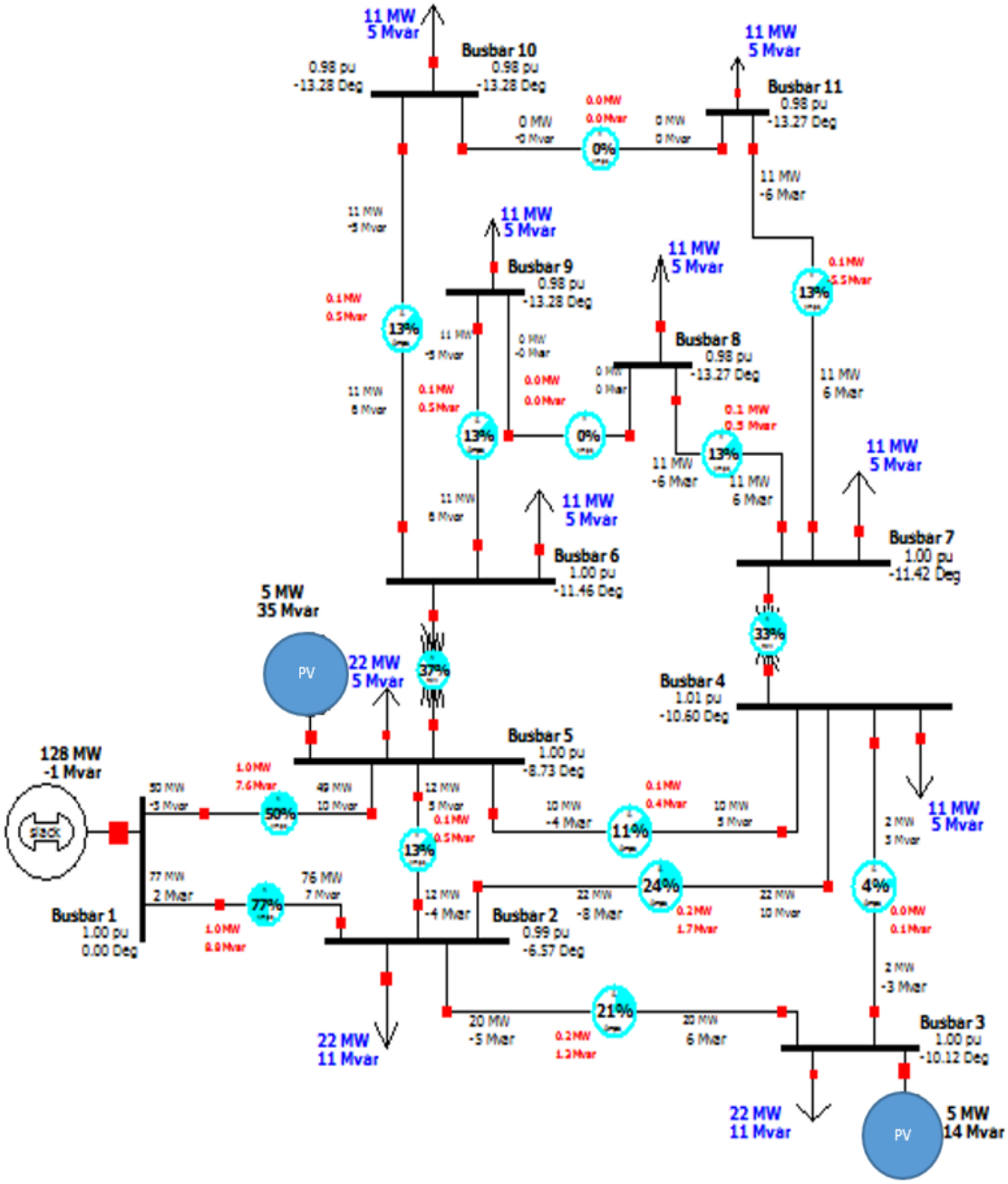

Figure 6.7: Simulation result of PV MODEL 2

6.8 The Improvement of System Efficiency

The improvement of system efficiency is a result of lower system losses and due to using a shunt capacitor as discussed below.

Table 6.7: Model explorer of PV MODEL 1 and PV MODEL 2

Name	Nom kV	PU Volt	Volt (kV)	Angle (Deg)	Load MW	Load MVar	Gen MW	Gen MVar
PV MODEL 1								
Bus 1	138	1.00	138	0			127.95	21.08
Bus 2	138	0.98	135.37	-6.55	22.26	10.78		
Bus 3	138	1.00	138	-9.81	22.26	10.78	10	18.02
Bus 4	138	1.00	138.54	-10.72	11.13	5.39		
Bus 5	138	0.95	131.75	-8.9	22.13	5.39		
Bus 6	138	1.00	139.26	-11.89	11.00	5.00		
Bus 7	138	1.00	138	-11.71	11.00	5.00		
Bus 8	138	0.98	135.45	-13.58	11.13	5.39		
Bus 9	138	0.98	135.88	-13.64	11.13	5.39		
Bus 10	138	0.98	135.88	-13.64	11.13	5.39		
Bus 11	138	0.98	135.45	-13.58	11.13	5.39		
PV MODEL 2								
Bus 1	138	1	138	0			127.51	-0.74
Bus 2	138	0.99	136.76	-6.57	22.26	10.78		
Bus 3	138	1.00	138	-10.12	22.26	10.78	5	13.59
Bus 4	138	1.00	139.29	-10.6	11.13	5.39		
Bus 5	138	1.00	138	-8.73	22.13	5.39	5	34.88
Bus 6	138	0.99	137.81	-11.46	11	5		
Bus 7	138	1.00	138	-11.42	11	5	10	41.01
Bus 8	138	0.97	134.95	-13.27	11.13	5.39		
Bus 9	138	0.97	134.89	-13.28	11.13	5.39		
Bus 10	138	0.97	134.89	-13.28	11.13	5.39		
Bus 11	138	0.97	134.95	-13.27	11.13	5.39		

6.8.1 Analysis of Losses

PV MODEL 1 and PV MODEL 2 offered significant advantages over current power system (baseline scenario) in terms of lower losses, improved voltage profiles, reduced transmission loads, and reduced power outputs from the existing CCPP, which uses natural gas as the primary fuel. This section focuses on loss analysis where PV MODELs are superior compared to the existing power system of the baseline scenario. The results showed that there was no considerable difference in total losses between the existing system and PV MODEL 1, with a value of 2.6 MW or 1.8% of total power generated from the power plant. However, an increase in total losses with PV MODEL

2 (to the extent of 0.4 MW as compared to PV MODEL 1 and baseline) might be due to increased loads on transmission line 3 (Busbar 2 to 3) and transmission line 7 (Busbar 5 to 4) as the consequence of the addition of new PV power sources in Busbars 3 and 5.

6.8.2 Shunt Capacitor

Shunt capacitor can be used to improve the performance and efficiency of a power system [53]. It is due to the lowering of inductive reactance of the system and as such shunt capacitor can increase the power factor [53]. In the present study, a shunt capacitor with the capacity of 10 MVar directly reduces the total reactive power delivered to Busbar 3 (from 13 MVar of baseline scenario to 3 MVar), as shown in Figure 6.8. As is commonly known, additional power losses would lead to problems such as machine/turbine failures, heat-ups, and losses in the distribution system. However, in this study, the addition of shunt capacitor of 10 MVar does not directly affect the reduction of transmission losses.

6.9 Cost-Benefit Analysis

The foremost advantages of renewable energy are the absence of fossil cost and uncertainty of increases in conventional fossil fuel cost making this technology attractive. Moreover, PV power plant has low operational and maintenance cost compared to coal power plants [61]. It is a solid state power plant which is easy to install and expand and has the potential for a long lifetimes of over 20 years [62]. PV systems operate with high reliability and no pollution. These advantages make them suitable for remote or isolated locations. However, PV has a few disadvantages, which are high initial costs and low conversion efficiency (less than 20%) [63], compared to other conversion technologies such as gas turbine, coal-fired power plant, etc. As there was only one existing power generating unit in the region under study, economic

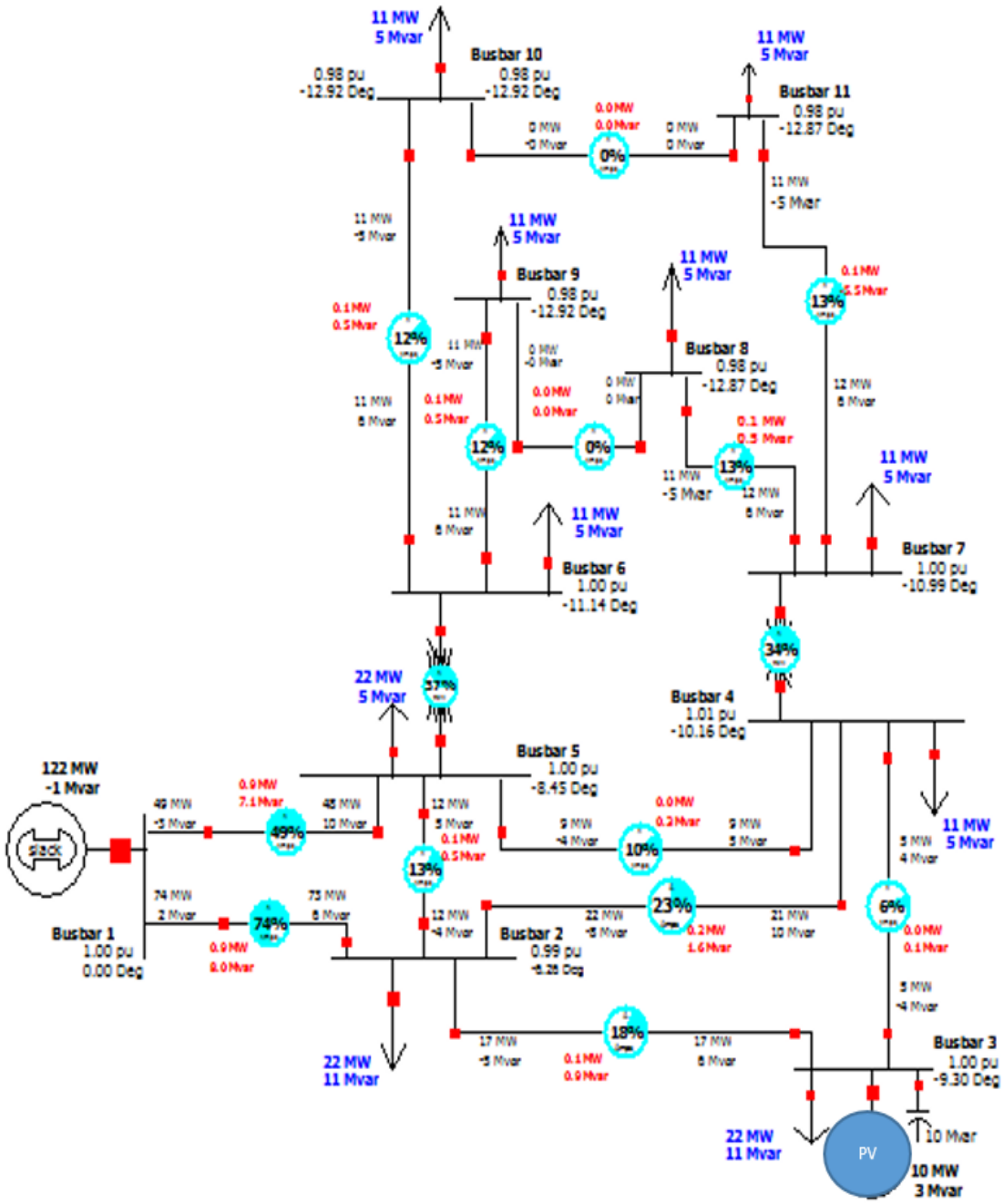

Figure 6.8: A shunt capacitor with a capacity of (10 MVar)

dispatch does not come into the picture as it typically focuses on the optimal output of a number of electricity generation facilities to meet the system load at the lowest possible cost, subject to transmission and operational constraints [53]. Instead, a cost-benefit analysis of installed PV power generation was considered.

Table 6.8: The cost-benefit analysis of PV MODEL to baseline scenario [62, 64, 46]

Code	Parameter	Value	Unit
A	Initial output capacity of CCPP	139	MW
B	Output capacity of CCPP	128	MW
C	Electricity price in Libya	0.5	USD/kWh
D	Interest rate in Libya	10%	
E	Electricity generation cost in Libya	15.39	USD/MWh
F	Natural gas price in Libya	4	USD/MMBtu
G	Annual solar availability	30%	
H	Power generation capital cost, PV	4183	USD/kW
I	CCPP heat rate	8500	Btu/kWh
J	Annual total hours	8760	Hours
K	Capital cost of PV power plant	4183	USD/kW
L	O&M Cost	27.75	USD/kW-yr.
M	Capacity of PV	10	MW
N	Capital cost (Yr.=0)	41,830,000	USD
O	O & M cost, PV	-277,500	USD
P	Losses reduction	0	MW
Q	Generation reduction of CCPP	1,482,980.40	USD
R	Sales of generation	14,454,000	USD
S	Total annual operating cost	15,659,480	USD
T	Payback period	2.67	years

With a capital cost of $4,183 USD/kW$ and Operational and Maintenance ($O\&M$) cost of $27.75 USD/kW - year$ [62], PV MODEL reduced the system losses and resulted in some economic advantages. In addition, with PV capital and $O\&M$ cost of $4,183/kW$ and $27.75 USD/kW - year$, the average electricity price of $0.5 USD/kWh$, a natural gas price of $4.0 USD/MMBtu$, the annual PV operating hours (solar availability) of 2,628 hours, and the combined cycle power plant (CCPP) heat rate of $8,500 Btu/kWh$, the payback period of the PV MODEL is estimated to be about 2.7 years, which is included in Table 6.8. Therefore, with high solar intensity reaching $8.1 kWh/m^2/day$ [65, 66], the construction of new PV power plants across the regions can bring economic benefits for both rural and urban areas of the country.

6.10 Socio-Environmental Impacts

Renewable Energy policies always provide opportunities for potential economic development and job creation. Previous studies have reported [46] solar PV has the highest job creating potential among all solar power technologies. Solar PV potentially creates 0.87 job-years per GWh, while CSP only generates 0.23 job-years per GWh. Therefore, if calculated, using 40% dedicated area for solar PV power plants and $8.1 kWh/m^2/day$ of solar intensity, the annual job creation could potentially reach 2800 jobs in the district of Al-kofra. In comparison to other renewable energy technologies (e.g. wind turbine, solar thermal, hydro, ocean, and biomass/waste power plants), PV power plants need the highest investment. It has been projected to substantially grow from nearly 1000 billion USD in 2010-2011 to 7000 billion USD in 2031-2040 globally [46]. According to Life Cycle Analysis (LCA) reported in [46], compared to natural gas, oil, and coal power plants (PPs), PV power plants considerably reduce GHG emissions; PV power plant emits 240 g CO_2-eq/kWh, while natural gas, oil, and coal PPs produce 900, 1100, and 1700 g CO_2-eq/kWh. Therefore, using PV MODEL, a 10 MW solar PV could favorably eliminate 6300 ton CO_2-eq of annual GHG emissions.

CHAPTER 7

OPTIMAL INTEGRATION OF PV GENERATION IN DISTRIBTION SYSTEMS

Integrating renewable energy such as solar PV generation into the grid has become more significant as an important part of the future network. Solar energy penetration level is highly site specific and readily available for modern power systems. Solar technologies are essentially pollution free and therefore available as the leading potential source of alternative energy. Moreover, cost of photovoltaic (PV) modules has been declining significantly at an average rate of 20% with each doubling of sales. Knowledge of available solar radiation in a location is a fundamental requirement before embarking on any solar energy project such as PV plants, solar thermal systems, and passive solar designs [67]. Integration of renewable energy based distributed generation sources (DGs) in a distribution system provides benefits such as relief in transmission, distribution capacity and enhancement of voltage profile [68]. A practical analysis of the impacts of grid connected DG units on system stability is presented in [69]. Authors of [70] presented an assessment of the impact of DG size and location under changing load condition due to a contingency on unbalanced distribution systems. The impact of DG capacity and location on voltage profile improvement of distribution systems has also been studied [71]. Distributed PV power generation has been growing rapidly in recent years. Due to the presence of clouds and their stochastic nature, integration of solar power could lead to supply demand imbalance, and subsequently pose significant challenges to the secure and reliable operation of a power system. Integrating renewable energy based distributed PV generation units

can have an impact on the practices used in distribution systems in the areas of power quality, stability, voltage profile, protection, power flow and reliability. Since DG units have a small capacity compared to central power plants, the impacts are minor if the penetration level is low (1%-5%). However, if the penetration level of DG units increases to the anticipated level of 20%-30%, the impact of DG units will be significant [72]. Voltage instability in distribution systems has been studied for decades and referred to as load instability [69]. For example, a voltage instability problem in a distribution network caused a major blackout in the S/SE Brazilian system in 1997 [73]. Optimal allocation of distributed PV generation units in a power network has become a significant factor for successful integration of renewable energy. In [74], a new method has been proposed to optimally allocate DG units to enhance the voltage profile at candidate buses by utilizing a voltage collapse index. However, the work fails to consider the impact of line outage. While in [75], authors utilized the outcome of the work in [74] to maximize loading under normal and contingency conditions. Distributed PV generation units must be integrated at optimal locations for maximum power system relief. An optimization technique to size and allocate renewable energy based distributed generation on distributed feeders factoring technical and economic constrains is proposed in [76]. Exploration of the effects of distributed generation units when small and substantial disturbances occur is discussed in [77]. The work in [71] considers minimization of voltage instability occurrences when DGs are placed at desirable locations in a power system. Techniques to optimally place DGs considering improvement of voltage profile and line loss reduction have been introduced in [75].

7.1 Impact of Integrating PV System on Voltage Profile

The impact of distributed PV generation on voltage profile and stability has become increasingly relevant. Issues such as voltage stability and voltage profile need to be

analyzed in detail. The failure of transmission lines to handle demand during peak times or contingencies may end in voltage instability leading to outages. Integration of renewable energy based distributed generation units with the distribution system can increase or decrease voltage stability depending on their operation. At present, most of the installed distributed generation operate at unity power factor to avoid interference with voltage regulation devices connected to the system [78, 79]. Appropriate location of DG units in distribution networks mitigates congestion in the lines and improves the voltage profile of the selected candidate buses in the network.

7.2 Calculation of PV Module Output Power

The variations of solar irradiance are statistically proven to follow a normal probability density function expressed as follows [32].

$$f(x) = \frac{1}{\sigma\sqrt{2\pi}} exp\left[- \frac{(x-\mu)^2}{2\sigma^2} \right] \tag{7.1}$$

Where x is the solar irradiance, μ and σ are the mean and standard deviation respectively [80]. The output power of PV module is dependent on the ambient temperature and the solar irradiance at the location as well as the characteristics of the module itself. Thus, the output power is calculated using the expression given below:

$$P_{say} = N * FF * V_y * I_y \tag{7.2}$$

$$FF = \frac{V_{MPP} * I_{MPP}}{V_{oc} * I_{sc}} \tag{7.3}$$

$$I_y = s\big[I_{sc} + K_i \times (T_{cy} - 25)\big] \tag{7.4}$$

$$V_y = V_{oc} - K_v \times T_{cy} \tag{7.5}$$

and

$$T_{cy} = T_A + s\left(\frac{N_{OT-20}}{0.8}\right) \tag{7.6}$$

where

P_{say}	output power of the PV module during state y;
N	Number of modules;
FF	Fill factor;
V_y	voltage during state y;
I_y	current during state y;
V_{oc}	Open-circuit voltage in V;
I_{sc}	Short-circuit current in A;
V_{MPP}	Voltage corresponding to the maximum power point;
I_{MPP}	Current corresponding to the maximum power point;
T_{cy}	Cell temperature $^{\circ}C$ during state y;
T_A	Ambient temperature $^{\circ}C$;
K_i	Current temperature coefficient $A/^{\circ}C$;
K_v	Voltage temperature coefficient $V/^{\circ}C$;
N_{OT}	Nominal operating temperature of cell in $^{\circ}C$;
S_{ay}	Average solar irradiance of state y;

The capacity factor of a PV module can be defined as the average output power divided by the rated power as expressed below [81].

$$CF_{PV} = \frac{P_{pv}^{Avag}}{P_{pv}^{rated}} \tag{7.7}$$

7.3 Load Uncertainty Modeling

Probabilistic power flow that accounts for load variability has been implemented in this chapter. For load uncertainty model the maximum load is placed at each load bus for all buses one at a time. For simplicity, the maximum load is assumed based on the desired loading conditions and the calculated mean and standard deviation of

the load. The probability density function (pr_n) for the load uncertainty is expressed as given below:

$$pr_n = \frac{1}{\sigma\sqrt{2\pi}} e^{-} \frac{(x-\mu)^2}{2\sigma^2} \tag{7.8}$$

where μ and σ are the calculated mean and standard deviation of assumed loads respectively.

7.4 Optimum Selection and Formulation of Voltage Index

The selection of candidate buses for distributed generation integration can be done randomly, by testing the voltage sensitivity to active power variation. This chapter focuses on the optimal allocation of the photovoltaic system based DG and improving the voltage profile of the distribution network. A voltage profile index is employed to test voltage sensitivity to load variation. The voltage index presented in [82, 83] has been used to determine the optimal allocation of PV system to improve the voltage profile of the system by using the formula below for a ten bus system:

$$V_{index} = \sum\nolimits_{n=1}^{10} \frac{V_n Pr_n}{10} \tag{7.9}$$

The highest voltage index indicates the optimal placement for the integration of distributed generation units for a 10 load bus system in terms of improving the voltage profile where V_n given as:

$$V_n = \frac{V_{candidateBus.withDGon}}{V_{candidateBus.withDGoff}} \tag{7.10}$$

The optimum location of the PV system in the distribution network is determined based on voltage index values obtained using these equations. The voltage index with the highest value corresponds to the optimum location and selected bus to integrate

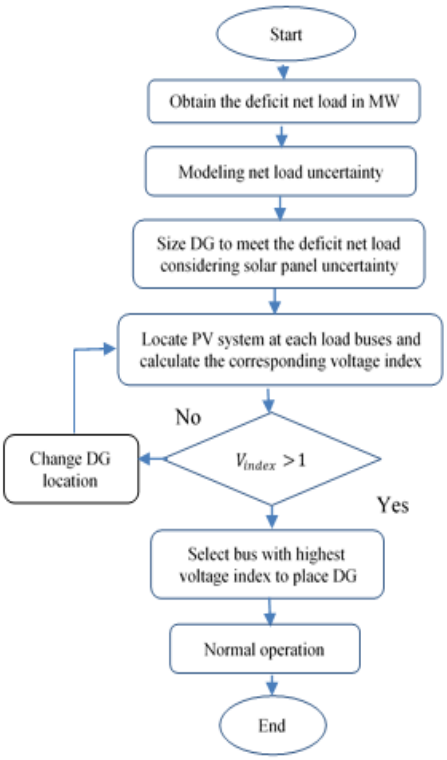

Figure 7.1: Flowchart for the proposed methodology

the distributed generation into the distribution network.

The impact of distributed generation (photovoltaic) integration into the distribution network is evaluated based on the following scenarios:

V_{index}<1, DG units will make the voltage profile worse.

$V_{index} = 1$, DG units will have no impact on the voltage profile.

V_{index}>1, DG units will improve the voltage profile.

With the proposed system consisting of distributed generation and by employing voltage index based on uncertainty load conditions, a complete voltage collapse can be mitigated. Simulation of the proposed system is illustrated by the flowchart shown in Figure 7.1

7.5 Results and Discussion

This section presents the simulation results using PowerWorld Simulator and Matlab. As mentioned earlier, the goal is the optimal integration of renewable energy based solar PV generation with the distribution network. The modified IEEE 12-bus radial system is used to test the proposed method. Bus 1 is the slack bus with a constant voltage of 1.05 per unit, and 0 angle, buses 2, 3, 4, 5, 6, 8, 9, 10, 11 and 13 are load buses as shown in Figure 7.2.The system has a total active power (P load) of 173.54 MW and reactive power (Q load) of 84.04 MVAR. The system's detailed line and load data are obtained from [50]. Integration of distributed photovoltaic generation into the existing distributed system with a maximum size of 10 MW (5% penetration level) at bus 13 is considered in this study as shown in Figure 7.3 . A probabilistic power flow that accounts for load uncertainty is implemented using equations (7.8), (7.9) and (7.10) to assess the voltage profile of the system.

The load uncertainty is modeled by placing the maximum loading condition of 31.12 MW and 17.07 MVAR once at every load bus as shown in Table 7.1. Results of bus variables also shown in Figures 7.4 and 7.5.

Table 7.1: Load Uncertainty Model

Bus No:	Max at Bus 2	Max at Bus 3	ax at Bus 4	Max at Bus 5	Max at Bus 6	Max at Bus 8	Max at Bus 9	Max at Bus 10	Max at Bus 11	Max at Bus 13
2	**31.12 MW**	22.26 MW	20.26 MW	13.13 MW	14.13 MW	30.12 MW	12.13 MW	11.13 MW	10.13 MW	9.13 MW
	17.07 Mvar	10.78 Mvar	8.78 Mvar	7.39 Mvar	5.39 Mvar	14.07 Mvar	6.39 Mvar	4.39 Mvar	2.39 Mvar	7.39 Mvar
3	9.13 MW	**31.12 MW**	22.26 MW	20.26 MW	13.13 MW	14.13 MW	30.12 MW	12.13 MW	11.13 MW	10.13 MW
	7.39 Mvar	**17.07 Mvar**	10.78 Mvar	8.78 Mvar	7.39 Mvar	5.39 Mvar	14.07 Mvar	6.39 Mvar	4.39 Mvar	2.39 Mvar
4	10.13 MW	9.13 MW	**31.12 MW**	22.26 MW	20.26 MW	13.13 MW	14.13 MW	30.12 MW	12.13 MW	11.13 MW
	2.39 Mvar	7.39 Mvar	**17.07 Mvar**	10.78 Mvar	8.78 Mvar	7.39 Mvar	5.39 Mvar	14.07 Mvar	6.39 Mvar	4.39 Mvar
5	11.13 MW	10.13 MW	9.13 MW	**31.12 MW**	22.26 MW	20.26 MW	13.13 MW	14.13 MW	30.12 MW	12.13 MW
	4.39 Mvar	2.39 Mvar	7.39 Mvar	**17.07 Mvar**	10.78 Mvar	8.78 Mvar	7.39 Mvar	5.39 Mvar	14.07 Mvar	6.39 Mvar
6	12.13 MW	11.13 MW	10.13 MW	9.13 MW	**31.12 MW**	22.26 MW	20.26 MW	13.13 MW	14.13 MW	30.12 MW
	6.39 Mvar	4.39 Mvar	2.39 Mvar	7.39 Mvar	**17.07 Mvar**	10.78 Mvar	8.78 Mvar	7.39 Mvar	5.39 Mvar	14.07 Mvar
8	30.12 MW	12.13 MW	11.13 MW	10.13 MW	9.13 MW	**31.12 MW**	22.26 MW	20.26 MW	13.13 MW	14.13 MW
	14.07 Mvar	6.39 Mvar	4.39 Mvar	2.39 Mvar	7.39 Mvar	**17.07 Mvar**	10.78 Mvar	8.78 Mvar	7.39 Mvar	5.39 Mvar
9	14.13 MW	30.12 MW	12.13 MW	11.13 MW	10.13 MW	9.13 MW	**31.12 MW**	22.26 MW	20.26 MW	13.13 MW
	5.39 Mvar	14.07 Mvar	6.39 Mvar	4.39 Mvar	2.39 Mvar	7.39 Mvar	**17.07 Mvar**	10.78 Mvar	8.78 Mvar	7.39 Mvar
10	13.13 MW	14.13 MW	30.12 MW	12.13 MW	11.13 MW	10.13 MW	9.13 MW	**31.12 MW**	22.26 MW	20.26 MW
	7.39 Mvar	5.39 Mvar	14.07 Mvar	6.39 Mvar	4.39 Mvar	2.39 Mvar	7.39 Mvar	**17.07 Mvar**	10.78 Mvar	8.78 Mvar
11	20.26 MW	13.13 MW	14.13 MW	30.12 MW	12.13 MW	11.13 MW	10.13 MW	9.13 MW	**31.12 MW**	22.26 MW
	8.78 Mvar	7.39 Mvar	5.39 Mvar	14.07 Mvar	6.39 Mvar	4.39 Mvar	2.39 Mvar	7.39 mvar	**17.07 Mvar**	10.78 Mvar
13	22.26 MW	20.26 MW	13.13 MW	14.13 MW	30.12 MW	12.13 MW	11.13 MW	10.13 MW	9.13 MW	**31.12 MW**
	10.78 Mvar	8.78 Mvar	7.39 mvar	5.39 Mvar	14.07 Mvar	6.39 Mvar	4.39 Mvar	2.39 Mvar	7.39 Mvar	**17.07 Mvar**

In Table 7.1, the first column refers to bus numbers and the subsequent ten

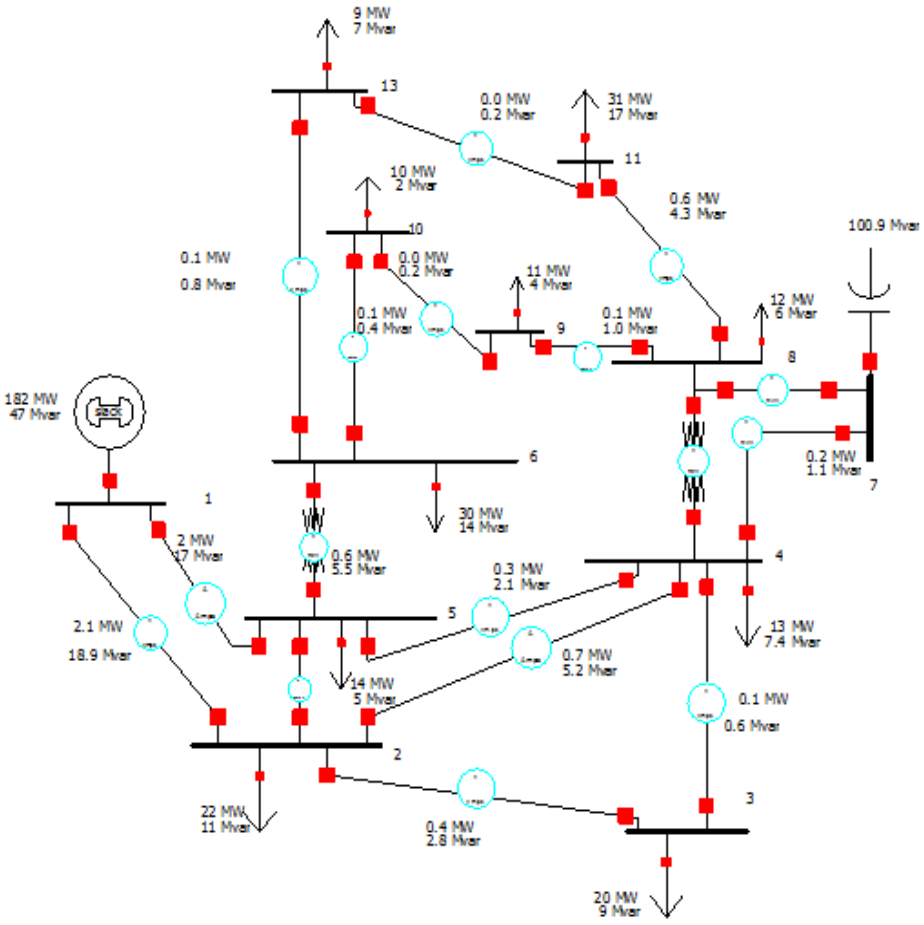

Figure 7.2: Distributed System under study (No PV)

columns refer to the scenario considered. The probability density function of each load in the 10 loading scenarios based on the load data in Table 7.1, are calculated using equation (7.8). Voltage index for the load buses has been calculated for voltage profile evaluation with the proposed system. The load flow results obtained after the simulation considering load uncertainty conditions are listed in Table 7.2

In order to investigate the optimal placement of distributed photovoltaic generation, voltage index is calculated at every bus considering the load uncertainty. The best location of distributed PV generation will give the highest voltage index as shown in Figure 7.6.

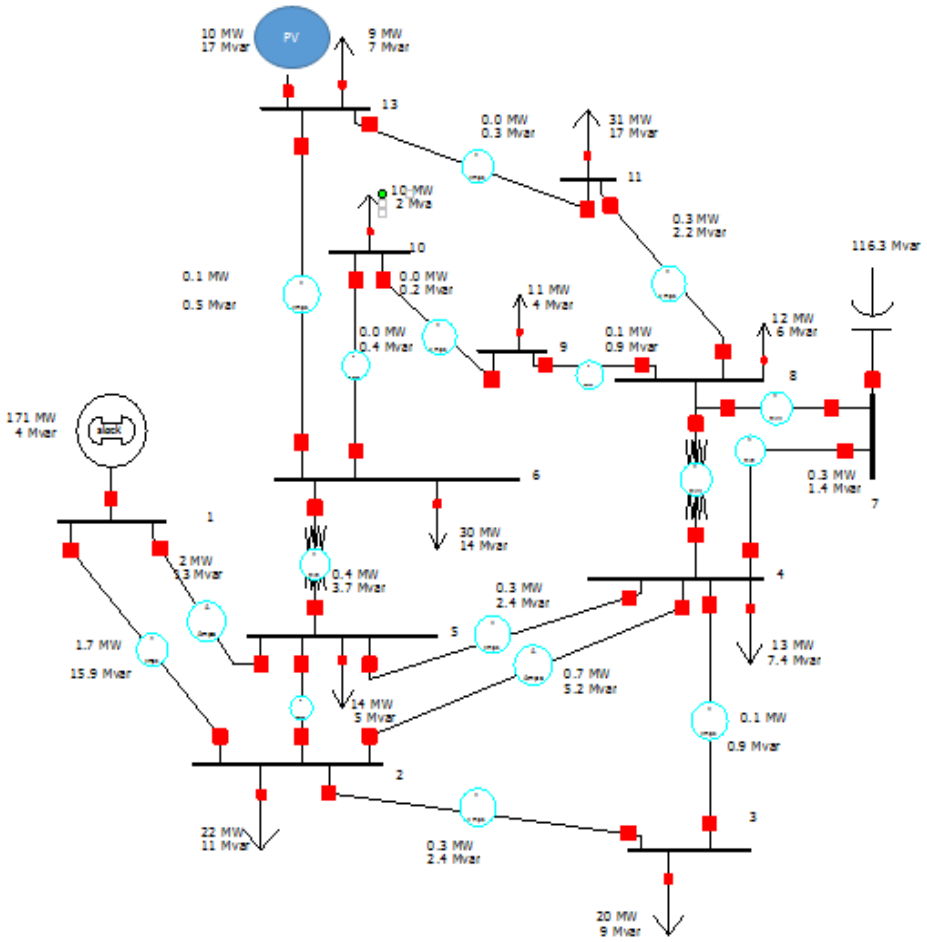

Figure 7.3: Distributed System with proposed PV

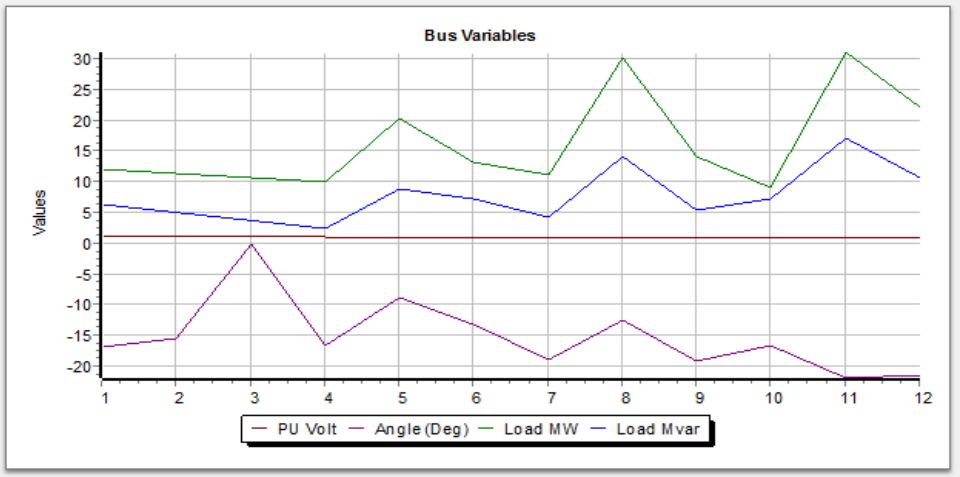

Figure 7.4: Simulation result of bus variables

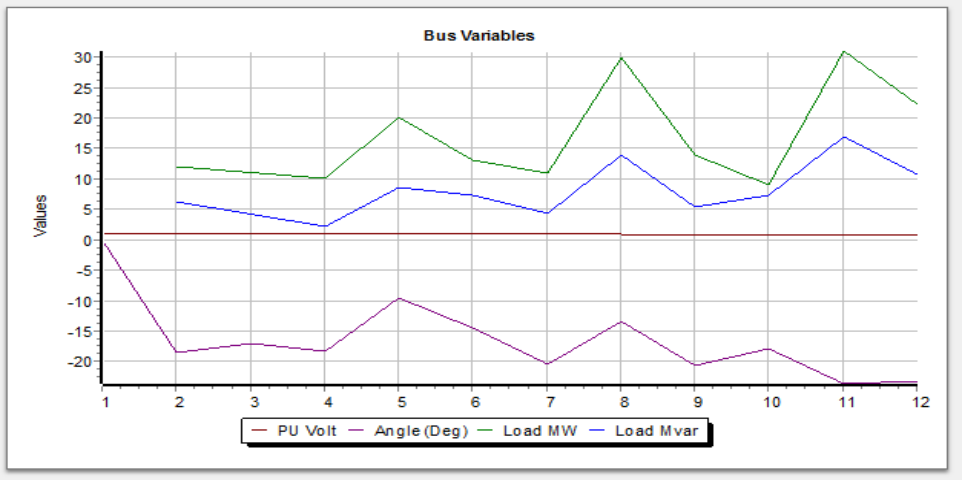

Figure 7.5: Simulation result of bus variables

Table 7.2: The voltage index values when DGs are installed at load buses

Bus No:	Vp.u at Bus 2	Vp.u at Bus 3	Vp.u at Bus 4	Vp.u at Bus 5	Vp.u at Bus 6	Vp.u at Bus 8	Vp.u at Bus 9	Vp.u at Bus 10	Vp.u at Bus 11	Vp.u at Bus 13	Voltage Index
2	0.9576	0.9437	0.9762	0.9502	0.9337	0.9798	0.9404	0.9272	0.9315	0.9417	1.0729
3	0.9597	0.9300	0.9734	0.9408	0.9169	0.9786	0.9064	0.8974	0.9201	0.9431	1.0605
4	0.9727	0.9546	0.9727	0.9321	0.8986	0.9775	0.9114	0.8724	0.9001	0.9287	1
5	0.9658	0.9640	0.9761	0.9229	0.8872	0.9769	0.9174	0.8898	0.8633	0.9050	1.0710
6	0.9649	0.9604	0.9769	0.9298	0.8847	0.9750	0.9073	0.8801	0.8756	0.8927	1.0581
8	0.9618	0.9562	0.9779	0.9470	0.9158	0.9768	0.9110	0.8930	0.9073	0.9298	1.0005
9	0.9623	0.9374	0.9745	0.9408	0.9071	0.9759	0.8850	0.8709	0.8928	0.9186	1.0148
10	0.9632	0.9552	0.9731	0.9338	0.8945	0.9767	0.9029	0.8602	0.8755	0.9056	1.0362
11	0.9612	0.9531	0.9758	0.9278	0.8943	0.9780	0.9318	0.8986	0.8529	0.8900	1
13	0.9607	0.9488	0.9757	0.9377	0.9020	0.9780	0.9351	0.9122	0.8821	0.8924	1.0764

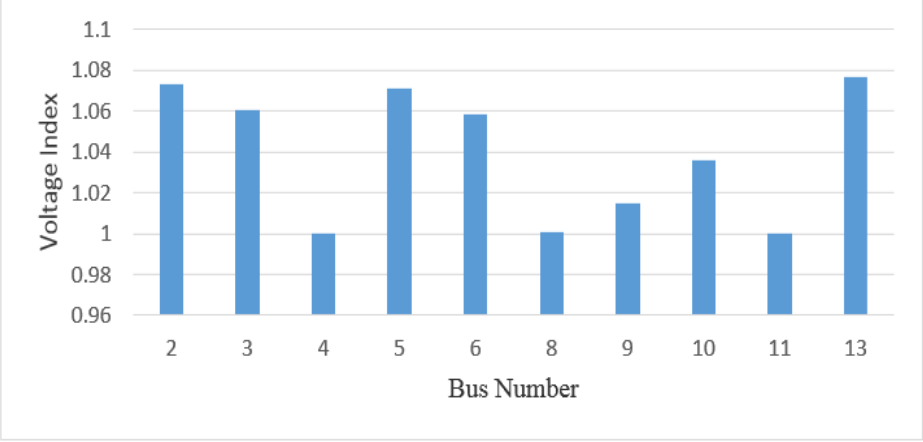

Figure 7.6: Variation of voltage index considering load uncertainty

CHAPTER 8

SUMMARY AND CONCLUDING REMARKS

The increasing energy demand in Libya can be largely provided by renewable energy, eliminating the need to build new fossil fuel power plant stations. An examination of grid-connected PV for the Libyan power system, especially its economic advantages, is very useful for utility companies. Solar and wind energy are considered to be the main sources of renewable energy in Libya. There is a need to attract investment in renewable technologies by enhancing the infrastructure and existing regulations for foreign investments. Entry of renewable energy technology is still in its early stages in Libya. A clear strategy and time plan is still needed to take this sector forward particularly in relation to developing the skills and knowledge needed for installation and maintenance of such systems.

8.1 Summary

In chapter 4, a study of the monthly insolation in Libya is presented. It will be very useful for those interested in large-scale entry of PV. In this study, probability density functions for modeling solar radiation in four locations in Libya have been discussed and the associated parameters are computed using four types of distribution functions. They are Weibull, Normal, Gamma and Rayleigh distribution. Two goodness of fit tests were used to identify the best fit at 5% level of significance, which are Chi-Squared test and Kolmogorov-Smirnov test. In addition Root Mean Square Error and Correlation Coefficient are used to determine the errors. It can be concluded that among those distribution models Weibull and Normal distribution give the best

fit for observed solar radiation.

A detailed study of grid-connected photovoltaics in the Libyan power system is aided by the massive dynamic of PV economics, as most of the companies can increase their revenues and/or lower their cost. It has been found that photovoltaics could provide an alternative source of energy and provide an opportunity to generate financial profits as well as decrease the consumption levels of oil and natural gas. The saved petroleum resources could be exported to bolster Libya's economy. In addition, the energy demand is increasing in Libya and PV could be the solution to cover some of this demand without the need to build new fossil fuel power plant stations due to the high availability of insolation amounting to about $8.1kWh/m^2/day$. The effect of integrating solar distributed generation into the grid results in a reduction of total amount of power generated by existing generation in the network. However, overall system losses obtained differ for the different scenarios, from 4.0 MW (scenario 1), 3.4 MW (scenario 2), 3.2 MW (scenario 3) and 2.1 MW (scenario 4). The results obtained using a 12 bus test distribution system indicated additional benefits with impacts on decision-making on integrating PV units into the power system. The inclusion of these benefits in the study can lead to faster investment recovery with a high benefit to cost ratio and a short payback period.

In Chapter 6, the impact of integrating solar power generation (PV) into the existing power system at Al-Kofra power station is investigated. It is desired to enhance efficiency and system reliability measures by integrating distributed generation (PV) with the grid. Two scenarios of solar power generation were considered to analyze the impact of adding new PV to the existing system in the district of Al-Kofra using appropriate simulation techniques. The baseline scenario considered the existing power grid system that include 10 substations, 11 busbars and 13 transmission lines, while the PV MODEL scenario considered the utilization of large scale PV power plant (10 MW) in the district. The simulation found that the largest voltage drop

occurred at busbars 3 and 5. PV MODEL 1 considering the installment of all new PV solar power at busbar 3 resulted in an improvement of voltage profile (from 0.93 to 1.00 p.u) and a decrease of transmission load on transmission line 1 (in the range of 86% to 78%). It also reduces the transmission load on transmission line 2 (by about 57% to 52%), whereas PV MODEL 2 considered the placement of new PV power plant equally distributed (5 MW each) at busbar 3 and busbar 5. The results of PV MODEL 2 increases the voltage at busbar 3 (from 0.95 to 1.00 p.u) and busbar 5 (from 0.94 to 1.00 p.u). Furthermore, the total transmission losses of PV MODEL 1 and PV MODEL 2 were found to be 2.6 MW and 3.0 MW, accounting for 2.0% and 2.3% of total power generated from the power stations, respectively. The addition of a shunt capacitor rated at 10 MVar did not seem to result in a reduction of transmission losses. However, construction of a new PV power plant would reduce the annual consumption of natural gas by the existing power generation (CCPP) of 1.48 million USD, while it would also offer a payback period of 2.7 years. The current local supporting policies on renewably energy could significantly improve the penetration of solar PV across states in Libya, potentially generating 2800 jobs and reducing GHG emissions by about 6300 ton $CO_2 - eq$.

In chapter 7, this study considered a proper allocation of PV based on a probabilistic method of distributed generation units into the distribution system under load uncertainty conditions to improve the voltage profile of the system. Power flow simulations were performed including load variability. For load uncertainty model the maximum load is placed at each load bus one at a time for all buses. The candidate bus for the distributed generation installation is selected based on voltage sensitivity to active power variation. Simulation results show a significant improvement in voltage index and overall system operation when DG is optimally placed due to its ability to strategically inject real power.

8.2 Future Work

The approach to quantify some of the benefits of solar power can help designers to identify the best locations and ratings to connect solar PV plants to the existing power system to maximize the overall benefits. The following are some issues that have not been addressed in this study. They are recommended for future work based on this research.

- Transfer of knowledge related to renewable energy units to the local community, especially for those interested in the academic, industrial and service fields.
- Impact of different distribution of solar units in various sites all over Libya.
- Investigation of the effect of other renewable energy resources such as biomass and wind in combination with PV.
- Exploring the latest technologies in renewable energy and the potential of transferring such technologies appropriately to local prevailing conditions.
- Adopting renewable energy resources aided by natural gas can help Libya to become an exporter of energy in electrical form in addition to oil and gas in the Mediterranean region.
- Design a commercial simulation software for evaluation and economic analysis of solar power with particular reference to Libya.

REFERENCES

[1] M. Guarnieri, "The alternating evolution of dc power transmission [historical]," *IEEE Industrial Electronics Magazine*, vol. 7, no. 3, pp. 60-63, 2013.

[2] T. Blalock, "Monocyclic power: a novel but short-lived power distribution system," *IEEE Power and Energy Magazine*, vol. 3, no. 3, pp. 84-89, 2005.

[3] N. R. Council et al., Electricity from renewable resources: Status, prospects, and impediments. National Academies Press, 2010.

[4] A. Romson, "Swedens initiative challenges world to go fossil-free," Available online: www.government.se/.../2015/11/swedens-initiative-challenges-world-to-go-fossil-free/, 2016, [Online; accessed 26-November-2015].

[5] M. Andrei, "Costa Rica just ran 99% on renewable energy in 2015," Available online: https://www.zmescience.com/ecology/climate/costarica-renewable-energy-20122015/ , 2015, [Online; accessed 21-December-2015].

[6] T. C. R. Project, "How 11 countries are shifting to renewable energy," Available online: https://www.climaterealityproject.org/blog/ follow-leader-how-11-countries-are-shifting-renewable-energy, 2016, [Online; accessed 03-February-2015].

[7] R. Ren21 et al., "Global status report," Renewable energy policy network for the 21st century. Available online: http://www. ren21. net. Accessed, vol. 19, 2016.

[8] J. Wang, S. Yang, C. Jiang, Y. Zhang, and P. D. Lund, "Status and future strategies for concentrating solar power in china," *Energy Science & Engineering*, vol. 5, no. 2, pp. 100-109, 2017.

[9] T. W. Bank, "Worlds Largest Concentrated Solar Plant Opened in Morocco," Available online: http://www.worldbank.org/en/news/press-release/2016/02/04/worlds-largest-concentrated-solar-plant-opened-in-morocco, 2016, [Online; accessed 23-March-2018].

[10] J. L. Sawin, F. Sverrisson, K. Seyboth, R. Adib, H. E. Murdock, C. Lins, I. Edwards,M. Hullin, L. H. Nguyen, S. S. Prillianto et al., Renewables 2017 Global Status Report, 2013.

[11] F. CIA, "The world factbook," Available online: https://www.cia.gov/library/publications/the-world-factbook, 2010.

[12] RCREEE, "Country Profile Renewable Energy in Libya 2012," Available online: http://www.rcreee.org/wp-content/uploads/2013/05/RCREEE CountryProfileRE-2012-EN-Libya.pdf, 2012, [Online; accessed May-2013]

[13] GECOL, "General Electrical Company of Libya 2010," Available online: `http://www.energyafrica.de/leadmin/userupload/EnergyAfrica13/PresentationGECOLAshaibiPAnel\%204a7th\%20German-African\%20Energy\%20Forum.pdf,2010`

[14] I. M. Saleh, "Prospects of renewable energy in libya," *in Solar Physics and Solar Eclipses (SPSE 2006)*, 2006, pp. 153-161.

[15] RCREEE, "Provision of Technical Support/Services for an Economical, Technological and Environmental Impact Assessment of National Regulations and Incentives Renewable Energy and Energy Efficiency," Available online: http://www.rcreee.org/, 2016.

[16] M. R. Patel, Wind and solar power systems: design, analysis, and operation. CRC press, 2005.

[17] F. Trieb, "Project manager for the trans-csp and the associated aqua-csp and med-csp report," Available online: www. trecuk. org. uk/reports. htm, 2011.

[18] M. Ekhlat, I. , and N. Kreama, "Energy efficiency and renewable energy. libya-national study," Sophia Antipolis: UNEP, Plan Bleu, Regional Activity Centre, 2007.

[19] C. E. Backus, "Solar cells," New York, *IEEE Press*, 1976. 511 p, 1976.

[20] M. Mrohs, Photovoltaic Technology and System DesignTraining Manualcation, 1988.

[21] T. Markvart, Solar electricity. John Wiley & Sons, 2000, vol. 6.

[22] O. S. Heavens, Optical properties of thin solid lms. Courier Corporation, 1991.

[23] A. Fahrenbruch and R. Bube, Fundamentals of solar cells: photovoltaic solar energy conversion. Elsevier, 2012.

[24] K. Ro, "Two-loop controller for maximizing performance of a grid-connected photovoltaic-fuel cell hybrid power plant," Ph.D. dissertation, Virginia Tech, 1997.

[25] H. S. Rauschenbach, Solar cell array design handbook: the principles and technology of photovoltaic energy conversion. Springer Science & Business Media, 2012.

[26] NREL, "Photovoltaic: Basic Design Principles and Components," Available online: https://www.nrel.gov/docs/legosti/fy97/6981.pdf, 1997, [Online; accessed March-1997].

[27] W. M. Rohouma, "Reliability study of photovoltaic system (stand-alone)," Ph.D. dissertation, Tripoli University, 2003.

[28] F. Sick, Photovoltaics in buildings: a design handbook for architects and engineers. Routledge, 2014.

[29] P. James, Renewable Energy World, Jan-Feb-2004, No. 1, 6-7.

[30] H. Bulut and O. Buyukalaca, "Simple model for the generation of daily global solar-radiation data in turkey," *Applied Energy*, vol. 84, no. 5, pp. 477-491, 2007.

[31] T. P. Chang et al., "Investigation on frequency distribution of global radiation using different probability density functions," *International Journal of Applied Science and Engineering*, vol. 8, no. 2, pp. 99-107, 2010.

[32] A. Guwaeder and R. Ramakumar, "A study of the monthly insolation in libya," *in Technologies for Sustainability (SusTech)*, 2017 IEEE Conference on. IEEE, 2017, pp. 1-5.

[33] M. Boxwell, "Solar Electricity Hand Book 2017 Edition," Available online: http://solarelectricityhandbook.com/solarirradiance.html, 2017, [Online; accessed 5-May-2017].

[34] H. Rinne, The Weibull distribution: a handbook. Chapman and Hall/CRC, 2008.

[35] R. Ramakumar, Engineering reliability: fundamentals and applications. Prentice Hall, 1993.

[36] J. P. Hennessey Jr, "A comparison of the weibull and rayleigh distributions for estimating wind power potential," *Wind Engineering*, pp. 156-164, 1978.

[37] J. Seguro and T. Lambert, "Modern estimation of the parameters of the weibull wind speed distribution for wind energy analysis," *Journal of Wind Engineering and Industrial Aerodynamics*, vol. 85, no. 1, pp. 75-84, 2000.

[38] S. Miller and D. Childers, Probability and random processes: With applications to signal processing and communications. Academic Press, 2012.

[39] S. Singh and J. H. Taylor, "Statistical analysis of environment canada's wind speed data," *in Electrical & Computer Engineering (CCECE)*, 2012 25th IEEE Canadian Conference on. IEEE, 2012, pp. 1-5.

[40] T. T. Soong, Fundamentals of probability and statistics for engineers. John Wiley & Sons, 2004.

[41] A. Papoulis and S. U. Pillai, Probability, random variables, and stochastic processes. Tata McGraw-Hill Education, 2002.

[42] F. Almonacid, C. Rus, P. Perez, and L. Hontoria, "Estimation of the energy of a pv generator using artificial neural network," *Renewable Energy*, vol. 34, no. 12, pp. 2743-2750, 2009.

[43] G. Makrides, B. Zinsser, M. Norton, G. E. Georghiou, M. Schubert, and J. H. Werner, "Potential of photovoltaic systems in countries with high solar irradiation," *Renewable and Sustainable energy reviews*, vol. 14, no. 2, pp. 754-762, 2010.

[44] A. Asheibe and A. Khalil, "The renewable energy in libya: Present difficulties and remedies," in the Proceedings of the World Congress, 2013.

[45] A. Guwaeder and R. Ramakumar, "A study of grid-connected photovoltaics in the libyan power system," *Energy and Power*, vol. 7, no. 2, pp. 41-49, 2017.

[46] O. Edenhofer, R. Pichs-Madruga, Y. Sokona, K. Seyboth, S. Kadner, T. Zwickel, P. Eickemeier, G. Hansen, S. Schlomer, C. von Stechow et al., Renewable energy sources and climate change mitigation: Special report of the intergovernmental panel on climate change. Cambridge University Press, 2011.

[47] M. A. Eltawil and Z. Zhao, "Grid-connected photovoltaic power systems: Technical and potential problemsa review," *Renewable and Sustainable Energy Reviews*, vol. 14, no. 1, pp. 112-129, 2010.

[48] Z. Maheshwari and R. Ramakumar, "Smart integrated renewable energy systems (sires): A novel approach for sustainable development," Energies, vol. 10, no. 8, p. 1145, 2017.

[49] Z. M. Salameh, B. S. Borowy, and A. R. Amin, "Photovoltaic module-site matching based on the capacity factors," *IEEE transactions on Energy conversion*, vol. 10, no. 2, pp. 326-332, 1995.

[50] REAOL, "Hun 14 MW Photovoltaic Power Plant by REAOL, Libya," Available online: http://cdm.unfccc.int, 2012.

[51] Wikipedia, "City of Al-Kofra Libya," https://en.wikipedia.org/wiki/Kufra,Libya, 2017.

[52] C. Zuo, B. Wang, M. Zhang, M. A. Khanwala, and S. Dang, "Power flow analysis using powerworld: A comprehensive testing report," *in Fluid Power and Mechatronics (FPM)*, 2015 International Conference on. IEEE, 2015, pp. 997-1002.

[53] J. D. Glover, M. S. Sarma, and T. Overbye, Power System Analysis & Design, SI Version. Cengage Learning, 2012.

[54] O. A. Afolabi, W. H. Ali, P. Cofie, J. Fuller, P. Obiomon, and E. S. Kolawole, "Analysis of the load ow problem in power system planning studies," *Energy and Power Engineering*, vol. 7, no. 10, p. 509, 2015.

[55] PowerGen, "Turbine, 6b," https://powergen.gepower.com/products/heavy-duty-gas-turbines/6b-03-gas-turbine.html#0, 2017, [Online; accessed 30-April-2017].

[56] SNM, "Steam Turbine," http://www.snm.co.jp/products/turbines/haiatsu 01.html, 2017, [Online; accessed 30-April-2017].

[57] CSERS, High Solar Intensity for the region of Hoon, Tripoli, Libya, 2009.

[58] M. Nasr, Electric Power System of Libya and its Future, 2010.

[59] F. H. Alharbi and S. Kais, "Theoretical limits of photovoltaics efficiency and possible improvements by intuitive approaches learned from photosynthesis and quantum coherence," *Renewable and Sustainable Energy Reviews*, vol. 43, pp. 1073-1089, 2015.

[60] Trina, "Duo 60 Cell Module," http://static.trinasolar.com/sites/default/files/PS-M-0474%20A%20Datasheet Duomax PEG5.XX US Feb 2017 A.pdf, 2017, [Online; accessed 30-April-2017].

[61] U. EIA, "Capital cost estimates for utility scale electricity generating plants. us energy information administration (eia), washington dc, 201 pp," There is no corresponding record for this reference, 2016.

[62] U. EIA, "Updated capital cost estimates for utility scale electricity generating plants," US Energy Inf. Adm, vol. 524, 2013.

[63] P. Denholm and R. M. Margolis, "Evaluating the limits of solar photovoltaics (pv) in traditional electric power systems," *Energy policy*, vol. 35, no. 5, pp. 2852-2861, 2007.

[64] GECOL, General Electrical Company of Libya, Tripoli, 2010.

[65] F. CIA, "The world factbook," https://www. cia. gov/library/publications/the-world-factbook, 2016.

[66] S. P. Bindra and N. Salih, "Uncsd rio+ 20 libya national report future we want focal point on renewable in libya," *Natural gas*, vol. 6, pp. 20-7, 2014.

[67] H. Bulut and O. Buyukalaca, "Simple model for the generation of daily global solar-radiation data in turkey," *Applied Energy*, vol. 84, no. 5, pp. 477-491, 2007.

[68] P. Raja, M. P. Selvan, and N. Kumaresan, "Enhancement of voltage stability margin in radial distribution system with squirrel cage induction generator based distributed generators,"IET Generation, Transmission & Distribution, vol. 7, no. 8, pp. 898-906, 2013.

[69] R. Londero, C. Affonso, and M. Nunes, "Impact of distributed generation in steady state, voltage and transient stabilityreal case," *in PowerTech*, 2009 IEEE Bucharest. IEEE, 2009, pp. 1-6.

[70] S. Kotamarty, S. Khushalani, and N. Schulz, "Impact of distributed generation on distribution contingency analysis," *Electric Power Systems Research*, vol. 78, no. 9, pp. 1537-1545, 2008.

[71] N. G. Hemdan and M. Kurrat, "Distributed generation location and capacity effect on voltage stability of distribution networks," *in Student Paper, 2008 Annual IEEE Conference*. IEEE, 2008, pp. 1-5.

[72] Y. M. Atwa and E. El-Saadany, "Optimal allocation of ess in distribution systems with a high penetration of wind energy," IEEE Transactions on Power Systems, vol. 25, no. 4, pp. 1815-1822, 2010.

[73] R. Prada and L. J. Souza, "Voltage stability and thermal limit: constraints on the maximum loading of electrical energy distribution feeders," *IET Proceedings-Generation*, Transmission and Distribution, vol. 145, no. 5, pp. 573-577, 1998.

[74] H. Hedayati, S. A. Nabaviniaki, and A. Akbarimajd, "A method for placement of dg units in distribution networks," *IEEE transactions on power delivery*, vol. 23, no. 3, pp. 1620-1628, 2008.

[75] M. Alonso and H. Amaris, "Voltage stability in distribution networks with dg," *in PowerTech*, 2009 IEEE Bucharest. IEEE, 2009, pp. 1-6.

[76] B. Kroposki, P. K. Sen, and K. Malmedal, "Optimum sizing and placement of distributed and renewable energy sources in electric power distribution systems," *IEEE Transactions on Industry Applications*, vol. 49, no. 6, pp. 2741-2752, 2013.

[77] W. Freitas, J. C. Vieira, L. Da Suva, C. M. Affonso, and A. Morelato, "Long-term voltage stability of distribution systems with induction generators," *in Power Engineering Society General Meeting*, 2005. IEEE. IEEE, 2005, pp. 2910-2913.

[78] R. Walling, R. Saint, R. C. Dugan, J. Burke, and L. A. Kojovic, "Summary of distributed resources impact on power delivery systems," *IEEE Transactions on power delivery*, vol. 23, no. 3, pp. 1636-1644, 2008.

[79] H. Zeineldin, E. El-Saadany, and M. Salama, "Distributed generation microgrid operation: Control and protection," in Power Systems Conference: Ad-vanced Metering, Protection, Control, Communication, and Distributed Re- sources, 2006. PS'06. IEEE, 2006, pp. 105-111.

[80] J.-H. Teng, S.-W. Luan, D.-J. Lee, and Y.-Q. Huang, "Optimal charging/discharging scheduling of battery storage systems for distribution systems interconnected with sizeable pv generation systems," *IEEE Transactions on Power Systems*, vol. 28, no. 2, pp. 1425-1433, 2013.

[81] Y. Atwa, E. El-Saadany, M. Salama, and R. Seethapathy, "Optimal renewable resources mix for distribution system energy loss minimization," *IEEE Transactions on Power Systems*, vol. 25, no. 1, pp. 360-370, 2010.

[82] G. Nannapaneni, A. Amaniampong, T. M. Masaud, and R. Challoo, "Optimal allocation of scig and dfig based distributed generation considering load uncertainty and line outage: A comparative study," *in Innovative Smart Grid Technologies Conference (ISGT)*, 2016 IEEE Power & Energy Society. IEEE, 2016, pp. 1-4.

[83] R. Al Abri, E. F. El-Saadany, and Y. M. Atwa, "Optimal placement and sizing method to improve the voltage stability margin in a distribution system using distributed generation," *IEEE Transactions on power systems*, vol. 28, no. 1, pp. 326-334, 2013.

VITA

Abdulmunim Hadi Mabrouk Guwaeder

Candidate for the Degree of

Doctor of Philosophy

Dissertation: A STUDY OF THE PENETRATION OF PHOTOVOLTAICS INTO THE LIBYAN POWER SYSTEM

Major Field: Electrical and Computer Engineering

Biographical:

Education:

Completed the requirements for the Doctor of Philosophy in Electrical and Computer Engineering at Oklahoma State University, Stillwater, Oklahoma in December, 2018.
Completed the requirements for the Master of Science in Electrical and Computer Engineering at Newcastle University, Newcastle, England, UK in December, 2003.
Completed the requirements for the Bachelor of Science in Electrical and Electronics Engineering at the Higher Institute of Surman, Surman, Libya in December, 1992.

Experience:

Research Assistant at Engineering Energy Laboratory, School of Electrical and Computer Engineering, Oklahoma State University from January 2013 to Present.
Assistant Lecturer at School of Electrical and Computer Engineering, Surman, The Higher Institute of Surman from fall 2006 to December 2012.

Professional Memberships:

Department Representative, Graduate and Professional Student Government Association (GPSGA)
Student Member, Institute of Electrical and Electronics Engineers (IEEE)